Experimental results from the LHC.

CTEQ School, S. Glazov, 13 Sept 2021

LHC Standard Model tests

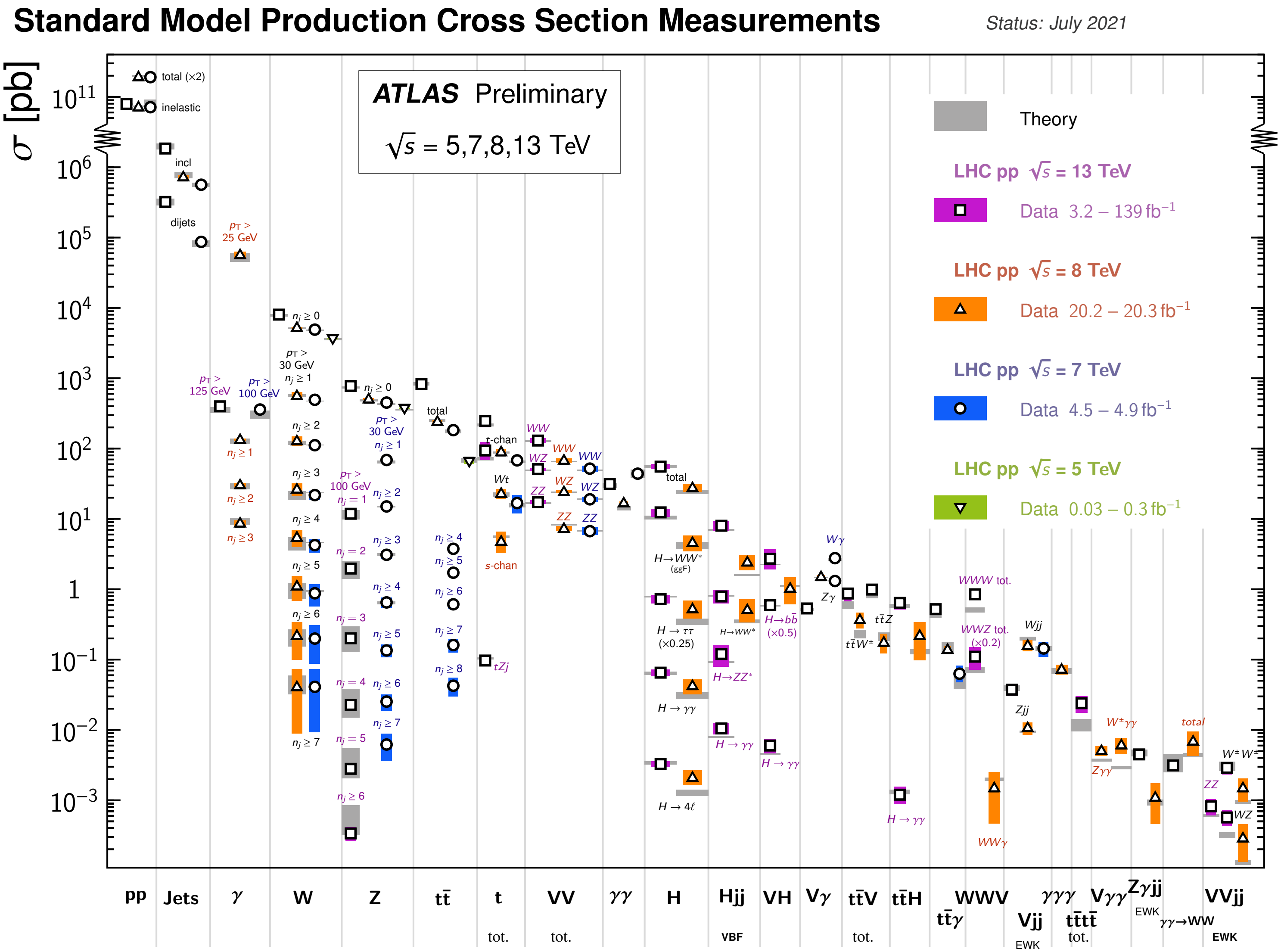

Many results covering a wide range of the Standard Model processes.

Precision tests of the Standard Model

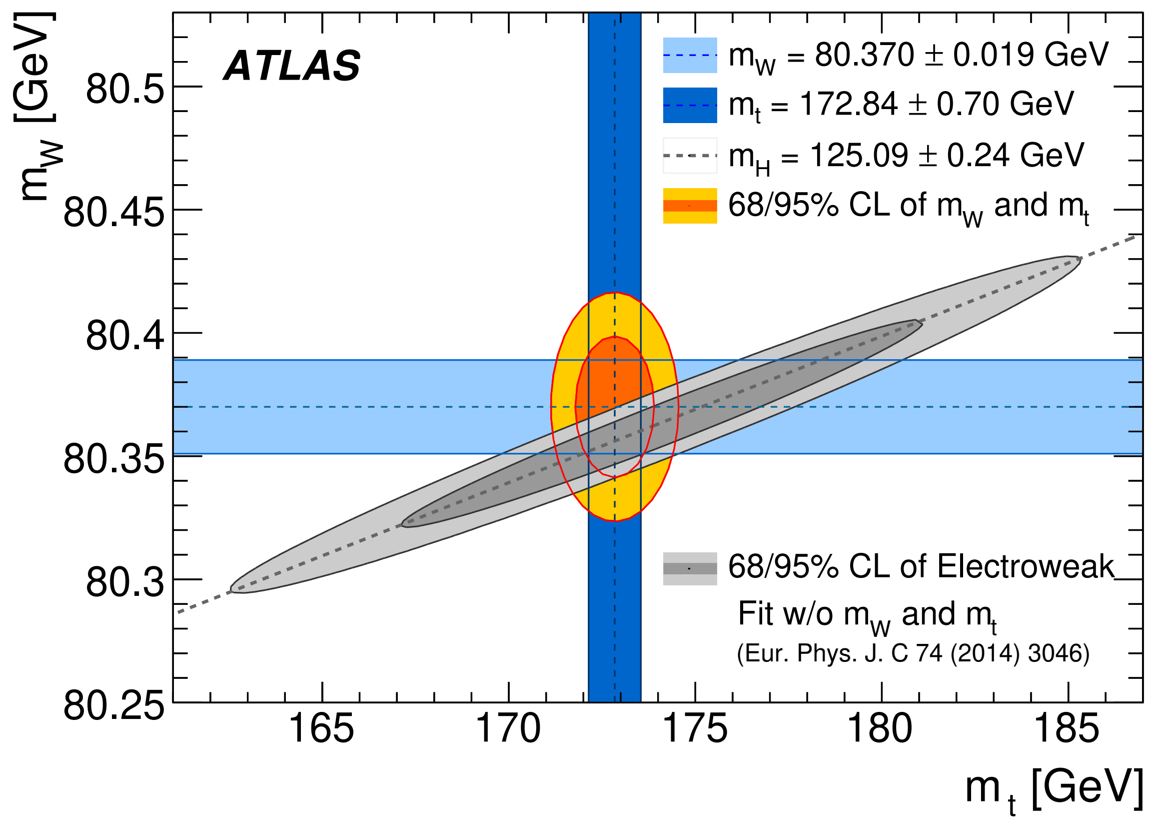

In these lectures, precision tests of the SM and Drell-Yan production are covered as an example. These measurements are also used as an example of experimental techniques and connection between the experiment and phenomenology.

Measurements of the M_W and $\sin^2\theta_W$

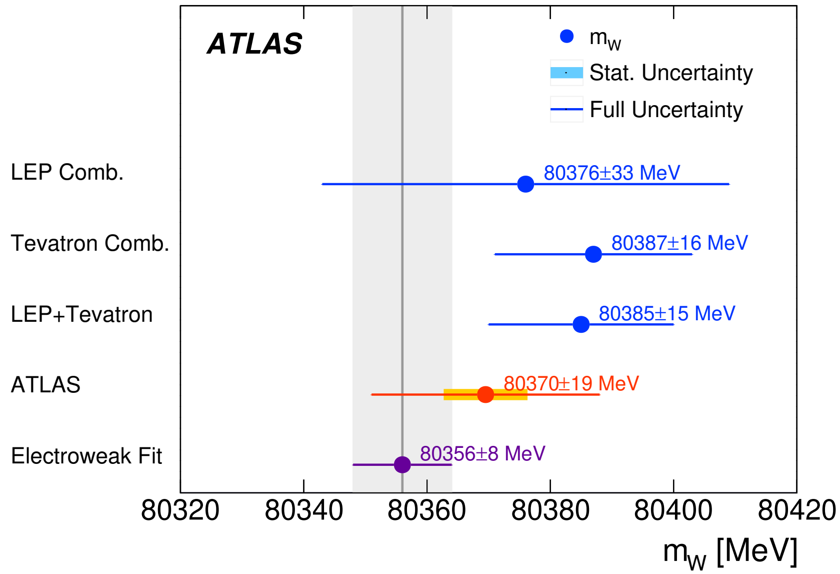

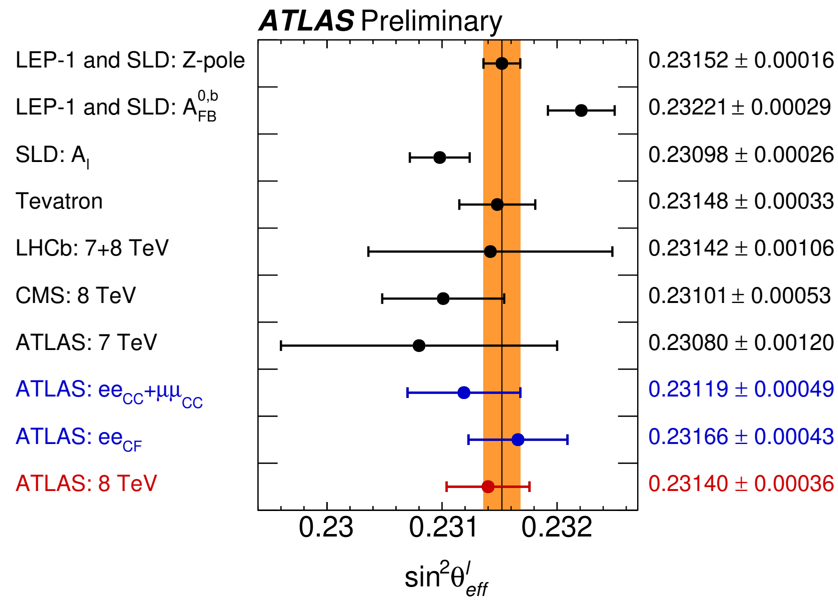

- LHC officially entered the precision electroweak race, with ATLAS, LHCb measurements of m_W and CMS of $\sin^2\theta_W$ using run-I data comparable to most accurate determinations from LEP/Tevatron.
- Leading uncertainties are from physics modelling: PDFs, recoil modeling, this will become worse for 13/14 TeV as the data start to probe lower x.
- $\rightarrow$ constrain them using experimental data.

ATLAS: EPJC 78 (2018) 110, CMS: EPJC 78 (2018) 701
ATLAS-CONF-2018-037

Drell-Yan process: LO production

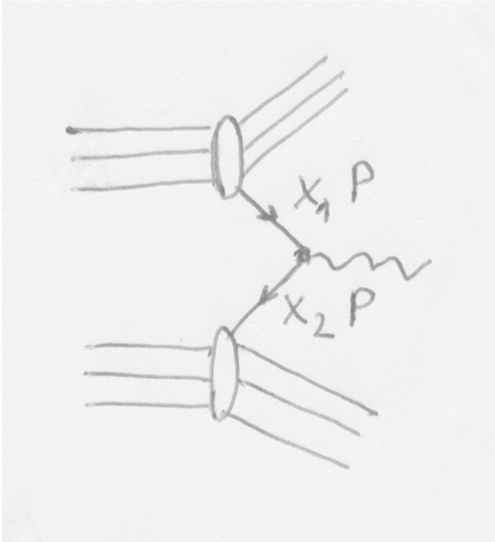

Drell-Yan process:

$$pp \to X + W, Z(\gamma) \to \ell\ell.$$

where $\ell\ell$ is ee, $\mu\mu$ and $\tau\tau$ pair for "neutral current" (NC) $Z(\gamma)$ exchange and $\ell\ell$ is $e\nu_e$, $\mu\nu_\mu$ and $\tau\nu_\tau$ for "charged current" (CC) W exchange.

The process can be classified in QCD as $2 \to 0$ — no colored particles in the final state. At LO, only $q\bar{q}$ annihilation contributes.

$\to$ simplest QCD process for pp colliders.

Drell-Yan process: LO kinematics

Consider x_1 and x_2 be fractions of the proton momenta carried by the partons participating in the interaction. At leading order, ignoring proton masses and transverse momentum,

$$M_{\ell\ell}^2 = (x_1\mathbf{P_1} + x_2\mathbf{P_2})^2 \approx x_1 x_2 S.$$

where $S = 4E_p^2$ is the center-of-mass energy squared and

$$y_{\ell\ell} = \frac{1}{2}\log\frac{E_{\ell\ell} + p_{Z,\ell\ell}}{E_{\ell\ell} - p_{Z,\ell\ell}} \approx \frac{1}{2}\log\frac{E_p(x_1+x_2) + E_p(x_1-x_2)}{E_p(x_1+x_2) - E_p(x_1-x_2)} = \frac{1}{2}\log\frac{x_1}{x_2}$$

Using these two formula, one can relate observable $M_{\ell\ell}$ and $y_{\ell\ell}$ with x_1, x_2:

$$x_{1,2} = \frac{M_{\ell\ell}}{\sqrt{S}} e^{\pm y_{\ell\ell}}.$$

Relation of *pp* and *ep* kinematics

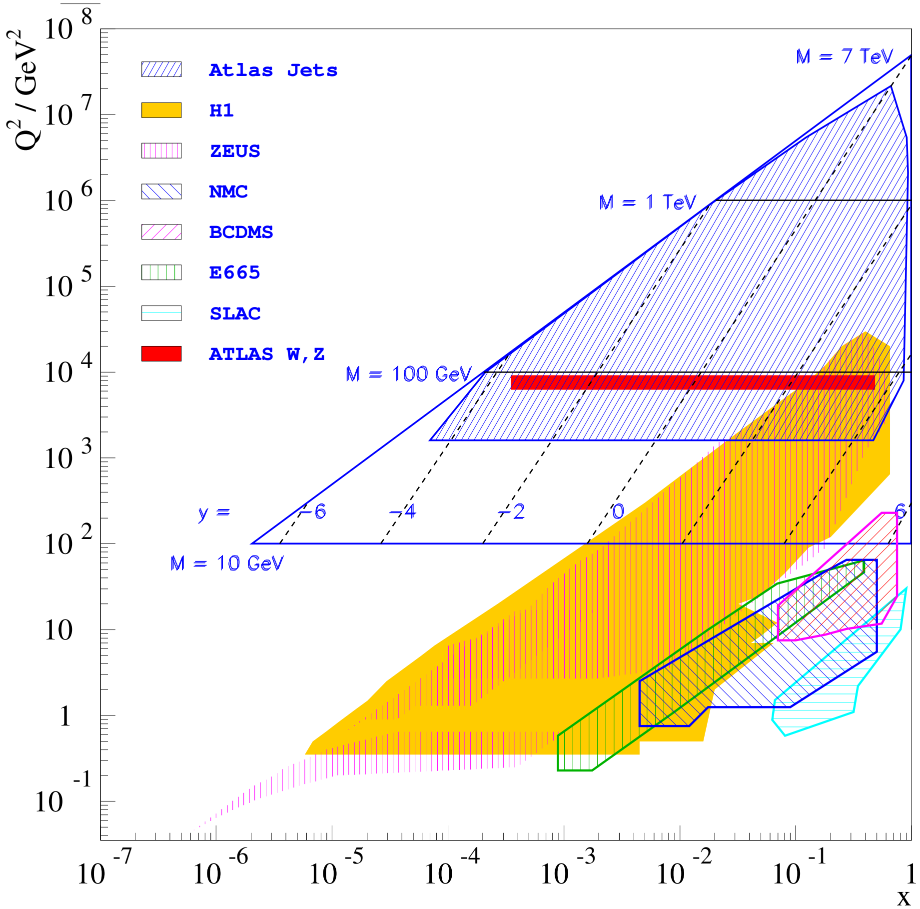

Measurements at *ep* and *pp* colliders cover a wide range in x and Q^2.
Measurements from HERA + pQCD evolution provide predictions for the LHC measurements range.

Neutral Current Drell-Yan Processes at the LHC

$$pp \rightarrow Xe^+e^-$$

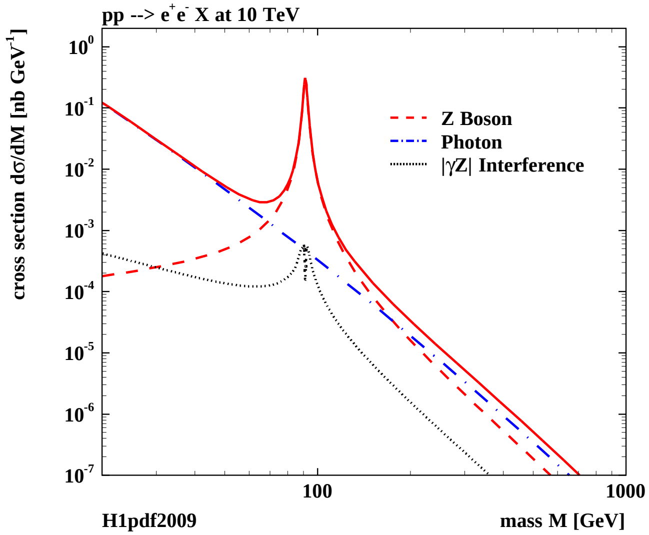

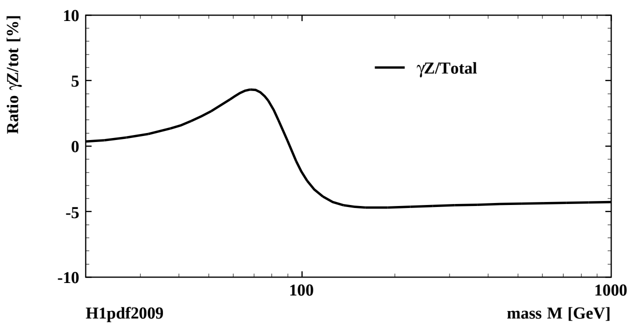

LO double differential cross section:

$$\frac{d^2\sigma}{dM_{\ell\ell}dy} = \frac{4\pi\alpha^2(M_{\ell\ell})}{9} \cdot M_{\ell\ell} \cdot P(M) \cdot \Phi(y, M_{\ell\ell}^2).$$

Propagator for γ exchange:

$$P_\gamma(M_{\ell\ell}) = \frac{1}{M_{\ell\ell}^4},$$

pure Z exchange:

$$P_Z(M_{\ell\ell}) = \frac{k_Z^2(v_e^2 + a_e^2)}{\left(M_{\ell\ell}^2 - M_Z^2\right)^2 + \Gamma_Z^2 M_Z^2},$$

where $k_Z = (4\sin^2\theta_W \cos^2\theta_W)^{-1}$, and γZ interference:

$$P_{\gamma Z}(M_{\ell\ell}) = \frac{k_Z v_e(M_{\ell\ell}^2 - M_Z^2)}{M^2\left[\left(M_{\ell\ell}^2 - M_Z^2\right)^2 + \Gamma_Z^2 M_Z^2\right]}.$$

Flavor decomposition of the Z production at the LHC

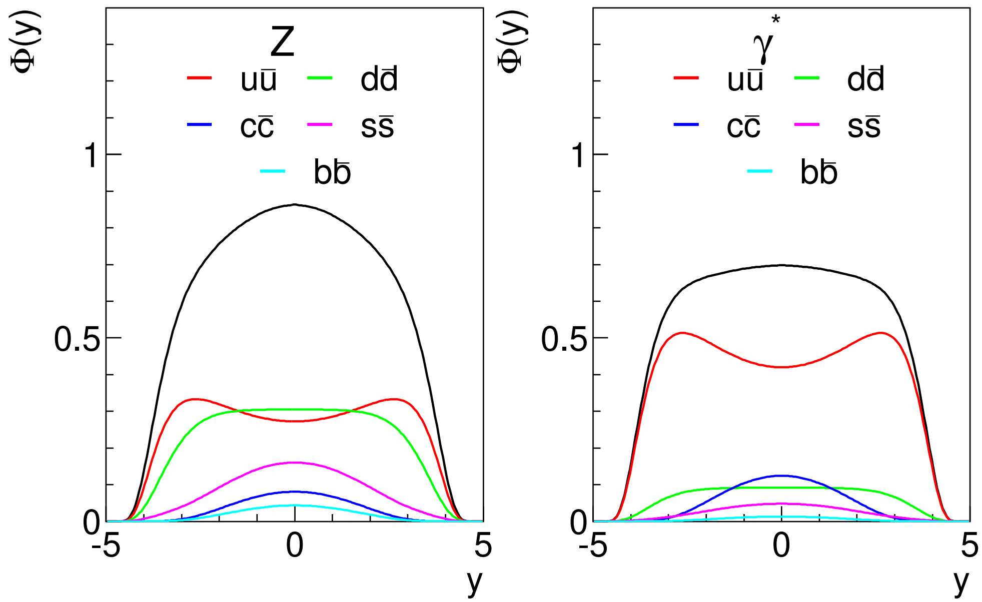

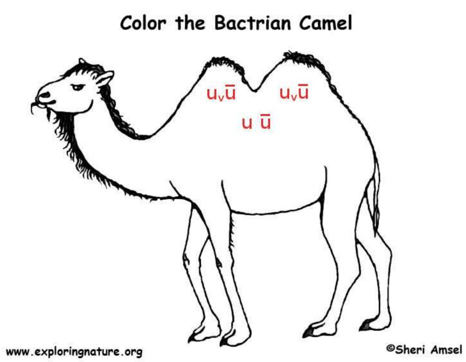

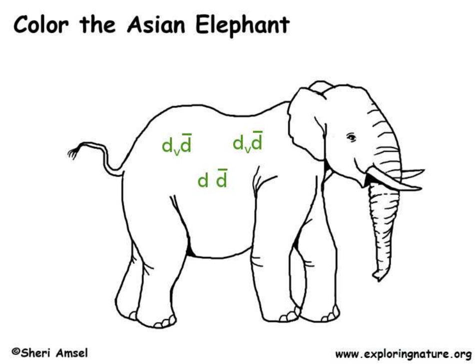

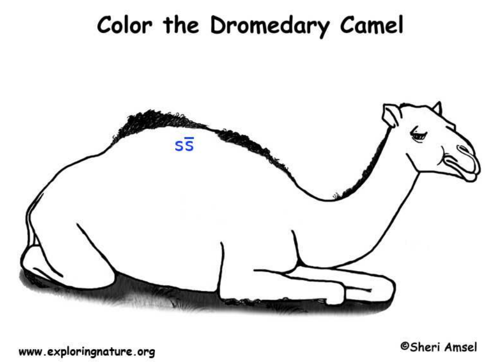

$\Phi(y, M^2_{\ell\ell})$ partonic structure is different for Z vs γ, with Z more sensitive to $d-$quarks. Rapidity distribution is also sensitive to partonic composition.

W^+ and W^- production flavour decomposition

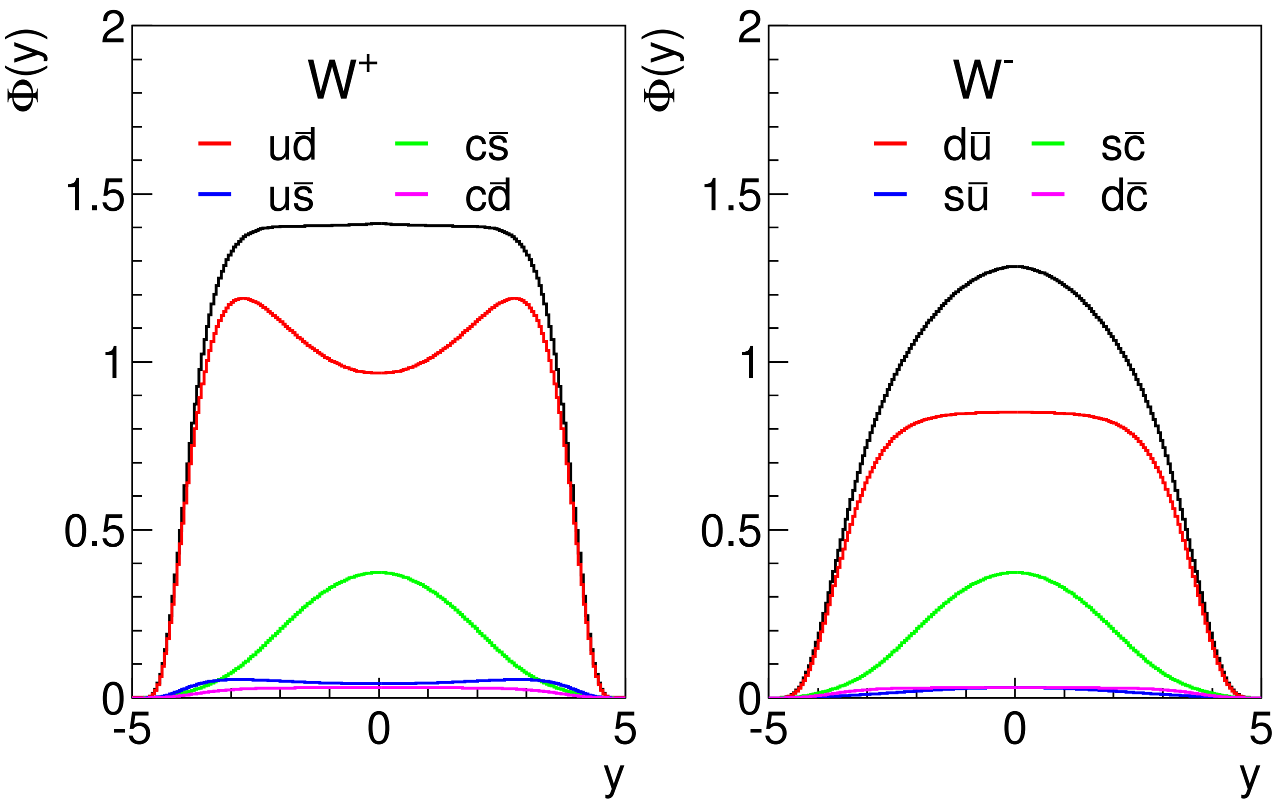

W^+ (W^-) production is sensitive to $u\bar{d}$ ($d\bar{u}$) as well as $c\bar{s}$ ($s\bar{c}$) flavour combinations and to lesser extend to Cabbibo suppressed pairs:

$$
\begin{aligned}
W^+ &\sim 0.95(u\bar{d} + c\bar{s}) + 0.05(u\bar{s} + c\bar{d}) \\
W^- &\sim 0.95(d\bar{u} + s\bar{c}) + 0.05(d\bar{c} + s\bar{u})
\end{aligned}
$$

W decays

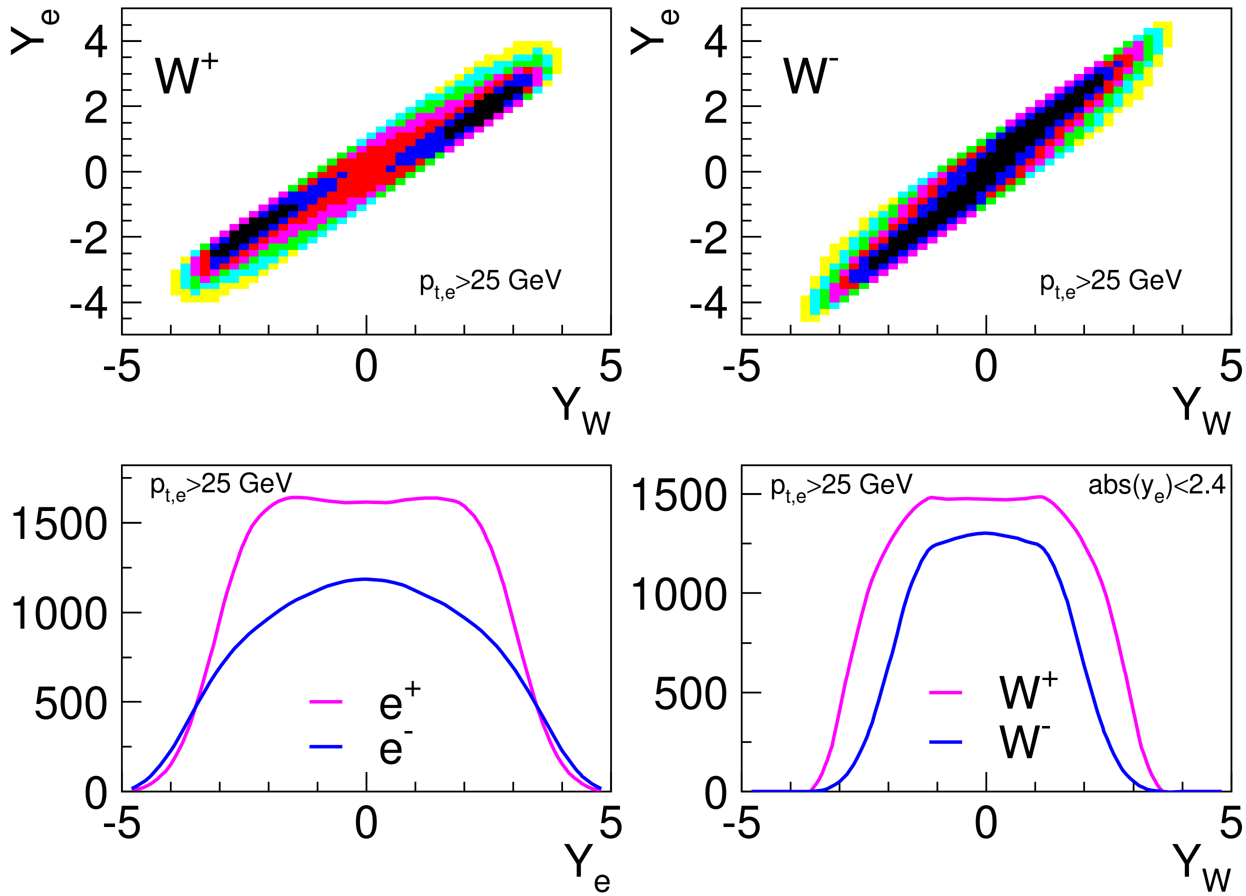

For $W^{\pm}$ production the observables are lepton p_t and η. V-A structure of the decay modifies rapidity distribution of the lepton vs the boson. W^+ production accesses higher y for a given η_e range.

(plots based on LO `MCFM`, HERAPDF1.0)

Recap

- Measurement of the W-boson mass require accurate modeling of the W-boson rapidity, transverse momentum and polarisation.
- Modelling needs control over flavour decomposition: $u, \bar{u}, d, \bar{d}, s, c$. Exotic $s - \bar{s}$ and intrinsic charm may play role too.
- Additional information is needed for $W\ p_T$.

$\rightarrow$ Obtain information using DY NN/CC data.

DY Event Reconstruction/Selection

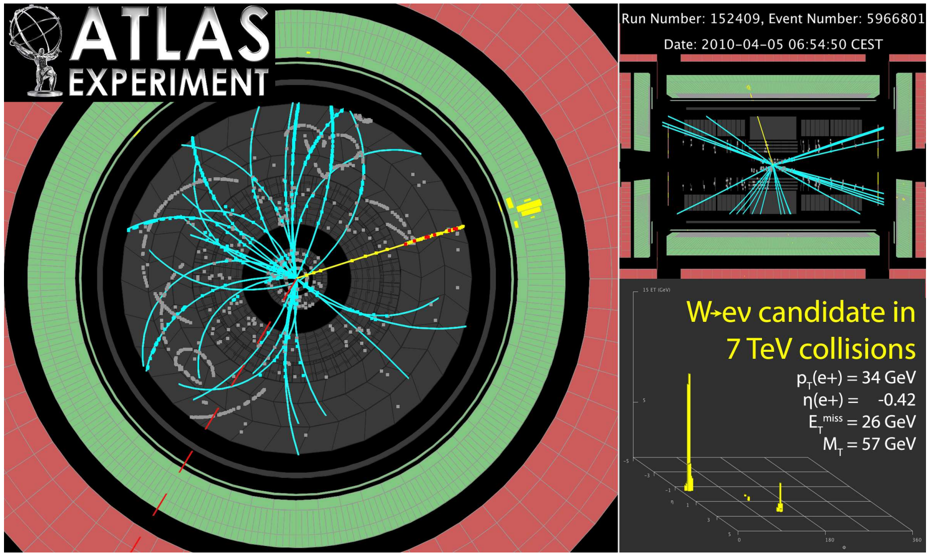

- Electron E_t, η: from calorimeter, inner detector.
- Muon P_t, η: from inner detector, muon system.
- E_t^{miss}: from combined HFS.

ATLAS	CMS
$E_{e,t}, p_{\mu,t} > 20$ GeV $\lvert\eta\rvert < 2.47$, Not $1.37 < \lvert\eta\rvert < 1.52$ (electrons) $\eta < 2.4$ (muons)	$E_{e,t}, p_{\mu,t} > 25$ GeV, $\lvert\eta\rvert < 2.5$ (electrons) $\lvert\eta\rvert < 2.1$ (muons)
Extra $W^{\pm}$ selection	
Veto extra electrons/muons $E_t^{\text{miss}} > 25$ GeV, $M_t > 40$ GeV	Veto extra electrons/muons
Extra Z selection	
$66 < M_{\ell\ell} < 116$ GeV	$60 < M_{\ell\ell} < 120$ GeV

Reconstruction of Electron(s) — Energy scale

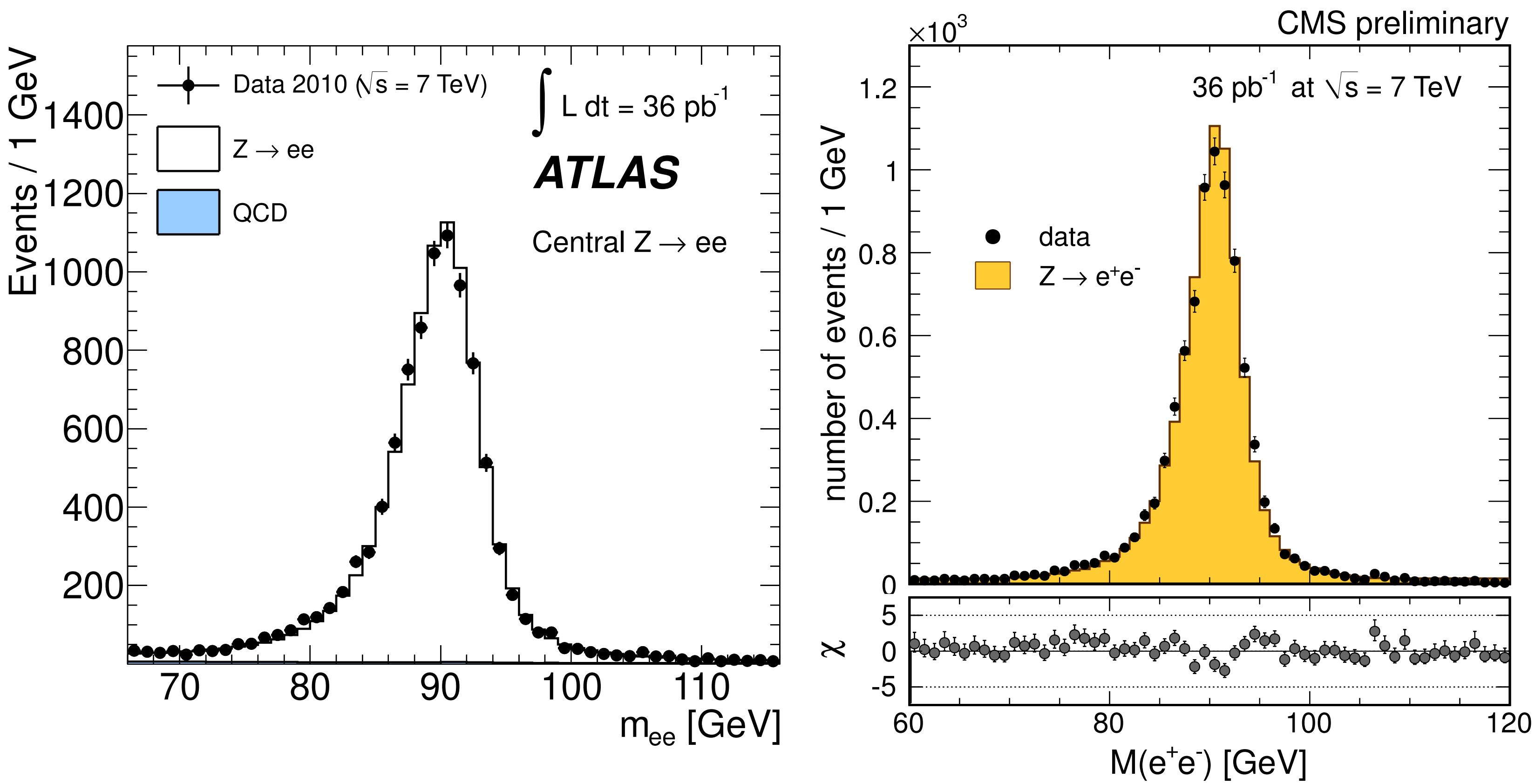

- Energy scale is important to reconstruct event kinematics.
- Calibrated using $Z \to e^+e^-$ events.
- Comparable resolution for ATLAS and CMS detectors.

Reconstruction of Muon(s) — Alignment and p_t scale

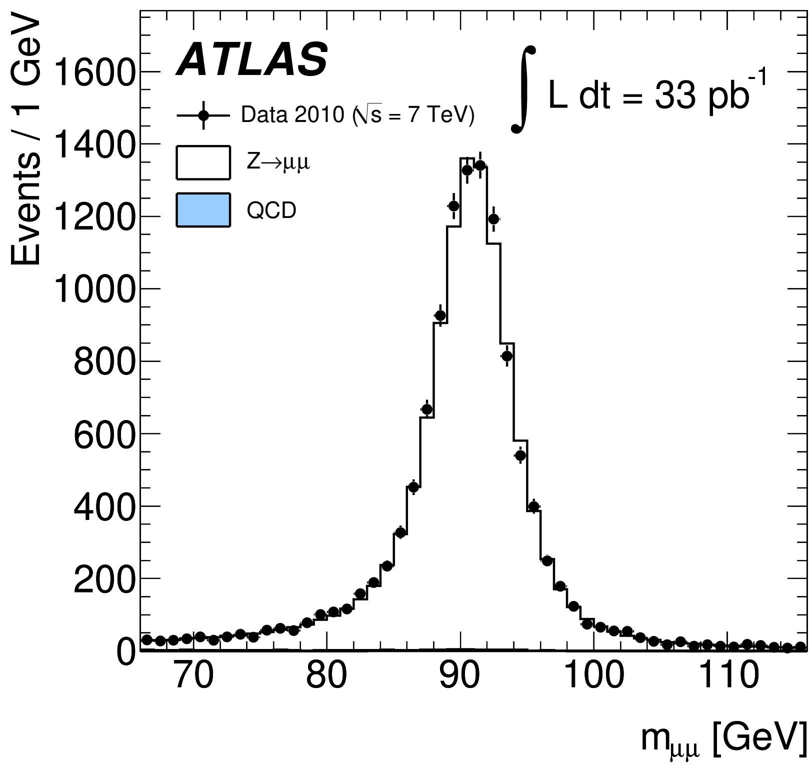

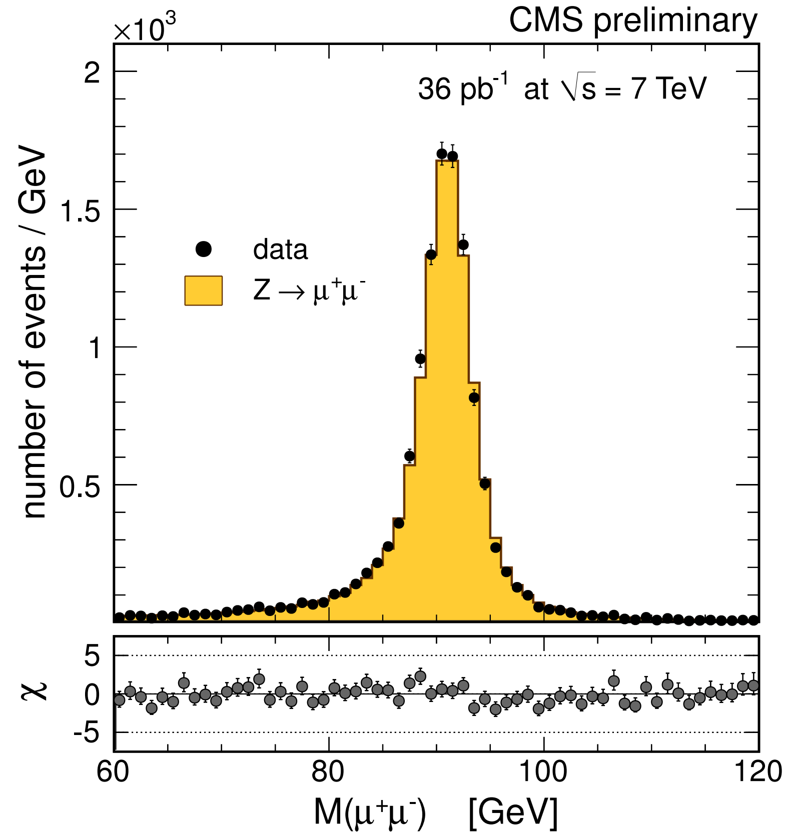

- Muon momentum reconstruction critically depends on detector alignment, checked by comparing inner detector/muon system standalone measurements.
- Comparable resolution for ATLAS and CMS detectors.

Background Determination for $W^{\pm} \to \ell^{\pm}\nu$ channels

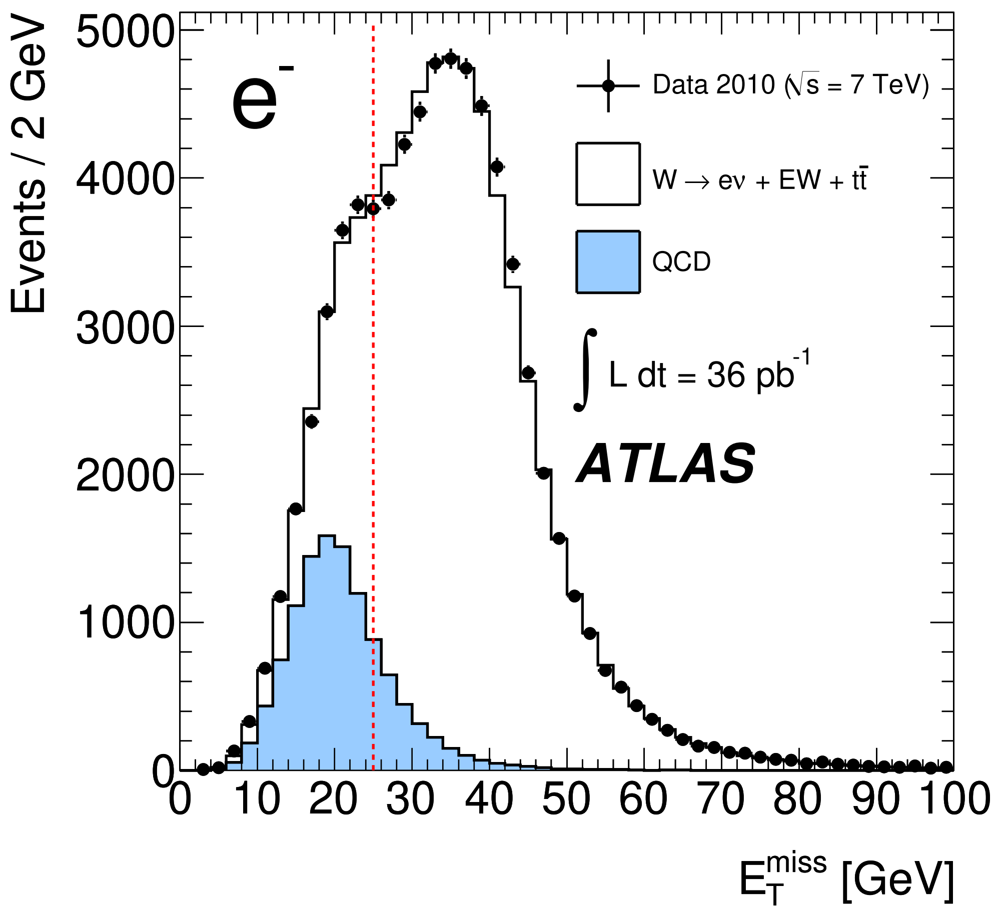

- Suppress QCD background by lepton identification/isolation cuts.
- Estimate EW background using MC simulation.
- Obtain data templates for QCD background: revert cuts to obtain pure BG sample.
- Fit data with MC + data driven background template.

After $E_t^{\mathrm{miss}} > 25$ GeV cut background level for ATLAS analyses is 4.3% for $W^- \to e^-\nu$, 2.6% for $W^+ \to e^+\nu$ and 1.7% for muon analyses.

Definition of fiducial measurements

The fiducial and total cross section measurements are defined as:

$$\sigma_{fid} = \frac{N_S - N_B}{C\mathcal{L}} \qquad \sigma_{tot} = \frac{\sigma_{fid}}{A}$$

where N_S, N_B are number of signal and background events and $\mathcal{L}$ is the integrated luminosity. Factors C and A are typically determined from MC:

$$C = \frac{N_{rec}^{cut}}{N_{gen}^{cut}} \qquad A = \frac{N_{gen}^{cut}}{N_{gen}}$$

where $N_{rec,gen}^{cut}$ is the number of events after fiducial cuts (e.g. $|\eta_\ell| < 2.5$) in reconstructed, generated signal events and N_{gen} total number of generated signal events. N_{gen}^{cut} can be defined differently with respect to (final state) QED radiation: "bare" (lepton only) "dressed" (photons combined with leptons using certain clustering method); and "born" (leptons taken before FSR).

Differential distribution unfolding

Since the particle detectors are not perfect, the observed distribution $F(X_{rec})$ is a convolution of the true distribution and detector response function:

$$F(X_{rec}) = \int T(X_{rec}, X_{gen}) F(X_{gen}) \mathrm{d}X_{gen} \,.$$

Unfolding is a procedure to determine $F(X_{gen})$ given observed in data $F(X_{rec})$ and T, that is normally obtained from MC (but other approaches, e.g. arXiv:1111.4896 exist). The unfolded distributions are typically discretized (“binned”). The unfolding procedure are typically regularized, but unregularized unfolding within profiled likelihood fits became more common recently.

Unfolding is an active area of recent developments. E.g. it is possible to unfold using several reco-level variables into single truth-level with ML methods, there are developments of un-binned unfolding.

For NC DY y_Z measurement, detector resolution is very good and there is little dependence on unfolding procedure.

Treatment of uncertainties

For large N_S, statistical uncertainties are estimated using normal distribution, this procedure is implicitly assumed for covariance matrix representation.

Systematic uncertainties are represented using nuisance parameters b_j or covariance matrix representation:

$$\chi^2(m_i, b_j) = \sum_i \left(\frac{m_i - (\mu_i + \sum_j \Gamma_{ij} b_j)}{\sigma_i} \right)^2 + \sum b_j^2, \qquad C_{ik} = \sum_j \Gamma_{ij} \Gamma_{kj} \, .$$

Care is required for multiplicative systematic uncertainties (e.g. luminosity measurement uncertainty) to avoid biases.

Input sources of systematics are usually assumed uncorrelated (e.g. energy scale vs PID efficiency). Many recent measurements profile uncertainties within unfolding (for example, by using control regions to fix background normalization), which correlates the sources.

Combination of different channels ($e-$ and $\mu-$) may lead to significant profiling of systematics.

Measurements in e and μ channels

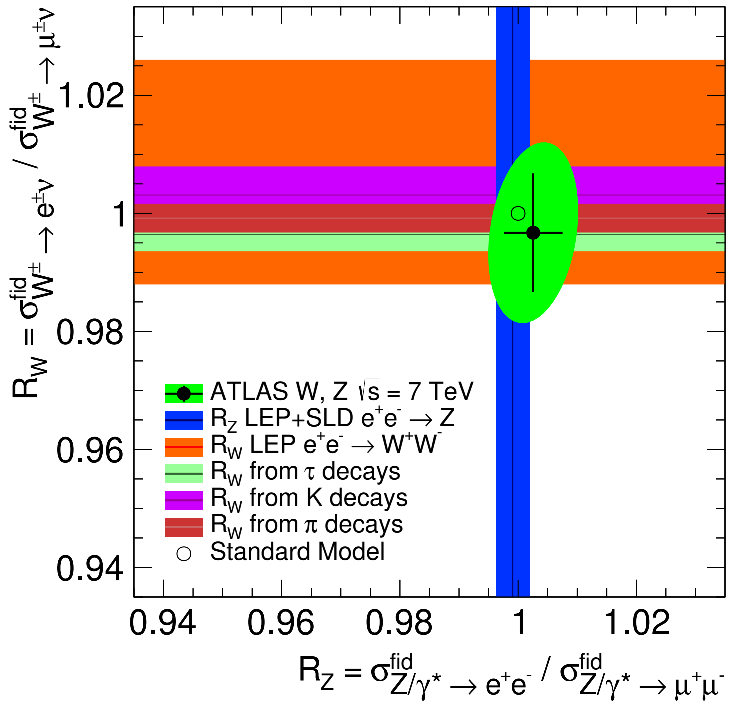

ATLAS EPJC 77 (2017) 367;
LEP+SLD, PR 427 (2006) 257;
HFAG arXiv:1412.7515;
KTEV PRD70 (2004) 092007;
NA62 PLB 719 (2013) 326;
PIENU PRL 115 (2015) 071801.

- Lepton universality for $Z \to \ell\ell$ probed to per mille accuracy at LEP, including $\Gamma_{Z\to\tau\tau}/\Gamma_{Z\to\ell\ell} = 1.0019 \pm 0.0032$.
- Lepton universality for $W \to e\nu$ and $W \to \mu\nu$ decays measured directly, controlled with high precision using π, K and τ decays.
- Relevant test given "B-anomalies". Interesting to test LUV using high mass DY, sensitive to non-universal Z'

W and Z cross sections at $\sqrt{s} = 7$ TeV

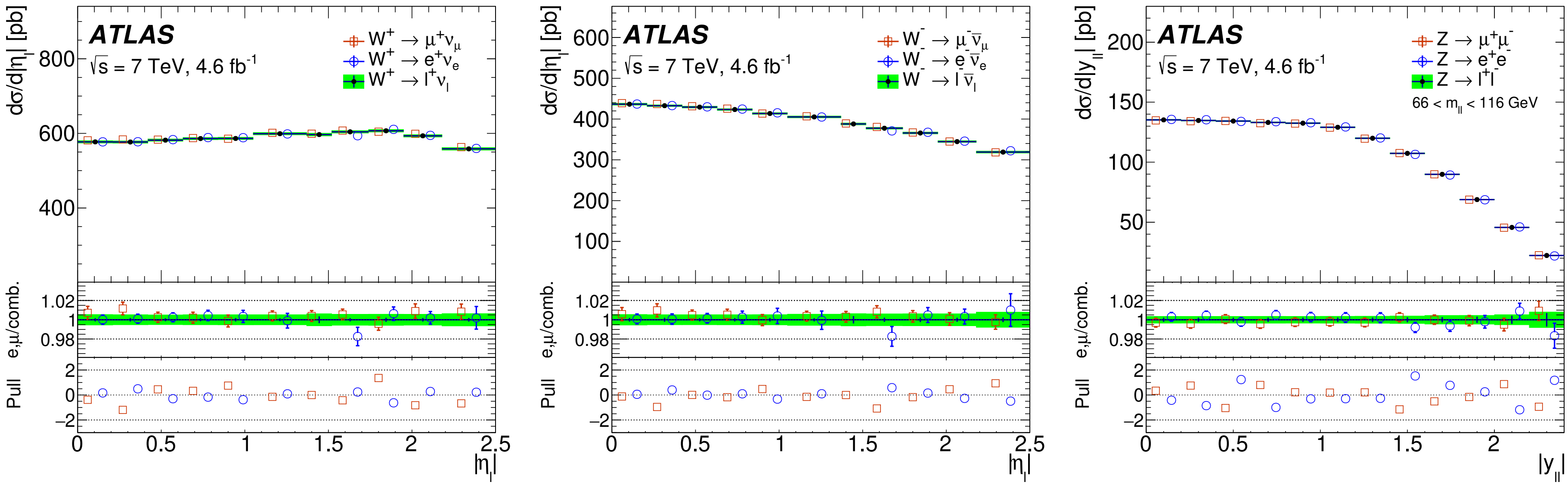

- Differential measurements of $W^{\pm}$, Z/γ^{*} production (including off-peak) using electron and muon decays, with sub-percent accuracy, and full correlated errors treatment.
- Good compatibility of the two channels, $\chi^2/\text{dof} = 47.2/44$, combined result has better than 0.5% accuracy.

ATLAS EPJ C77 (2017) 367.

W and Z cross sections at $\sqrt{s} = 7$ TeV

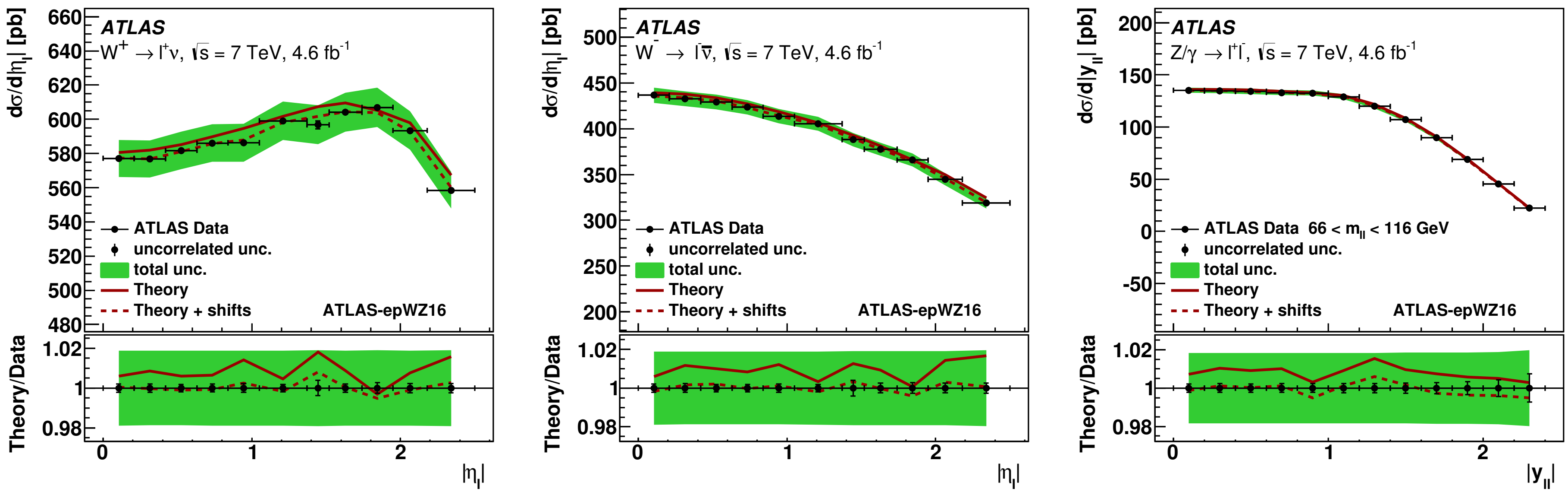

- ATLAS $W, Z/\gamma^*$ data together with the inclusive HERA-II data included in a QCD analysis at NNLO QCD + NLO EWK using xFitter program.
- Challenge for the theory to match the data accuracy, $\chi^2/\mathrm{N_{data}} = 108/61$ (ATLAS only) for the nominal scale settings $\mu_F = \mu_R = M_{\ell\ell}(M_W)$, improving to $\chi^2/\mathrm{N_{data}} = 85/61$ for $\mu_F = \mu_R = 1/2 M_{\ell\ell}(M_W)$

Effect of resummation

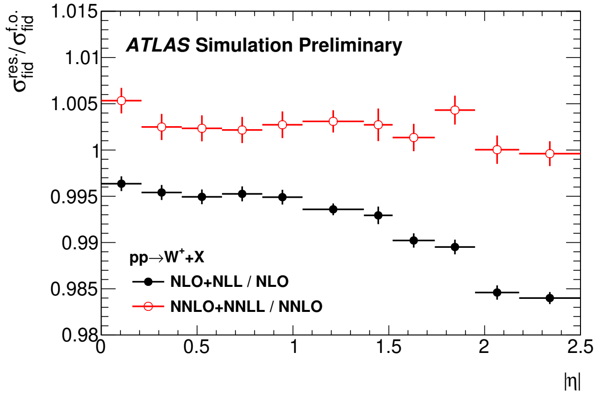

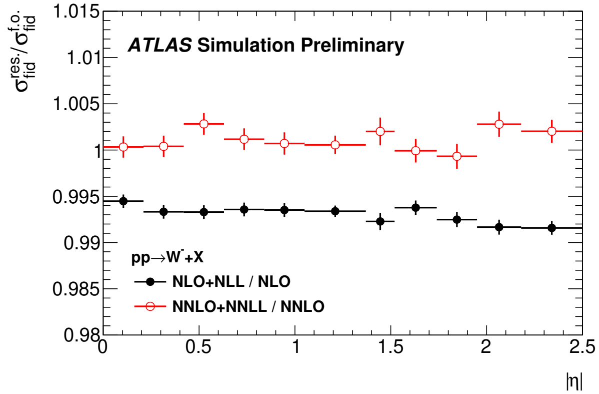

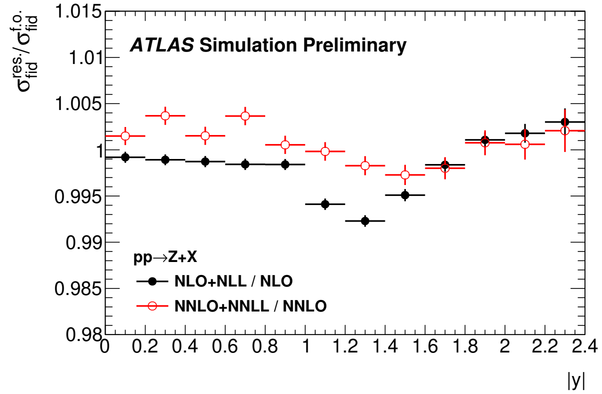

- 2011 W, Z differential cross section measurements are performed within fiducial volume, with $p_T^{\ell} > 20$ GeV and $E_T^{miss} > 25$ GeV cuts.
- Fiducial cuts shape $p_T^{W,Z}$ distribution, make fixed order predictions inaccurate.
- Difference observed between FEWZ and DYNNLO predictions for symmetric cuts (at $\sim 1\%$ level), however using asymmetric cuts does not solve the problem of p_T distribution shaping.
- Differences between NNLO and NNLO+NNLL calculations are comparable to data accuracy (but much better vs NLO - NLO+NLL).
- Differences for W^+ vs W^- – building asymmetry does not solve the problem completely.

ATL-PHYS-PUB-2018-004

Adding angular dependence

LO formula for NC DY including decay angle dependence:

$$
\begin{aligned}
P(M_{\ell\ell}, \cos\theta^*_{\ell\ell}) \quad &= e_\ell^2 e_q^2 (1 + \cos^2\theta^*) \\
&+ e_\ell e_q \frac{2m_{\ell\ell}^2 (M_{\ell\ell}^2 - M_Z^2)}{\sin^2\theta_W \cos^2\theta_W \left[(M_{\ell\ell}^2 - M_Z^2)^2 + \Gamma_Z^2 M_Z^2\right]} \left[v_\ell v_q (1 + \cos^2\theta^*) + 2a_\ell a_q \cos\theta^*\right] \\
&+ \frac{M_{\ell\ell}^4}{\sin^4\theta_W \cos^4\theta_W \left[(M_{\ell\ell}^2 - m_Z^2)^2 + \Gamma_Z^2 M_Z^2\right]} \left[(a_\ell^2 + v_\ell^2)(a_q^2 + v_q^2)(1 + \cos^2\theta^*)\right. \\
&\left. + 8a_\ell v_\ell a_q v_q \cos\theta^*\right].
\end{aligned}
$$

The decay angle $\cos\theta^*$ is typically measured in Collins-Soper frame:

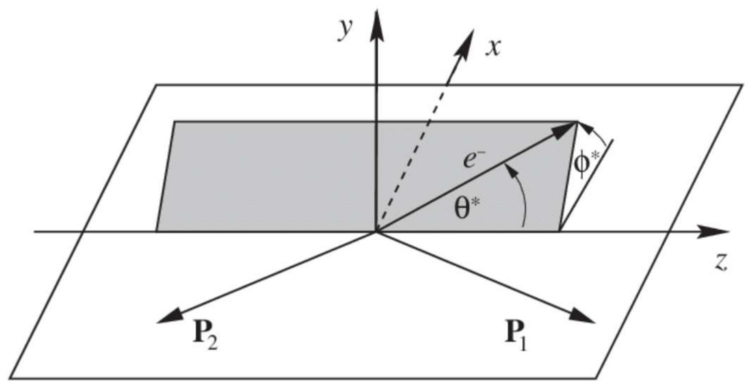

Terms linear in $\cos\theta$ enhance sensitivity to γZ interference and give access to $\sin^2\theta_W$.

Triple differential cross section $d^3\sigma/dM_{\ell\ell}d|y_{\ell\ell}|d\cos\theta^*$

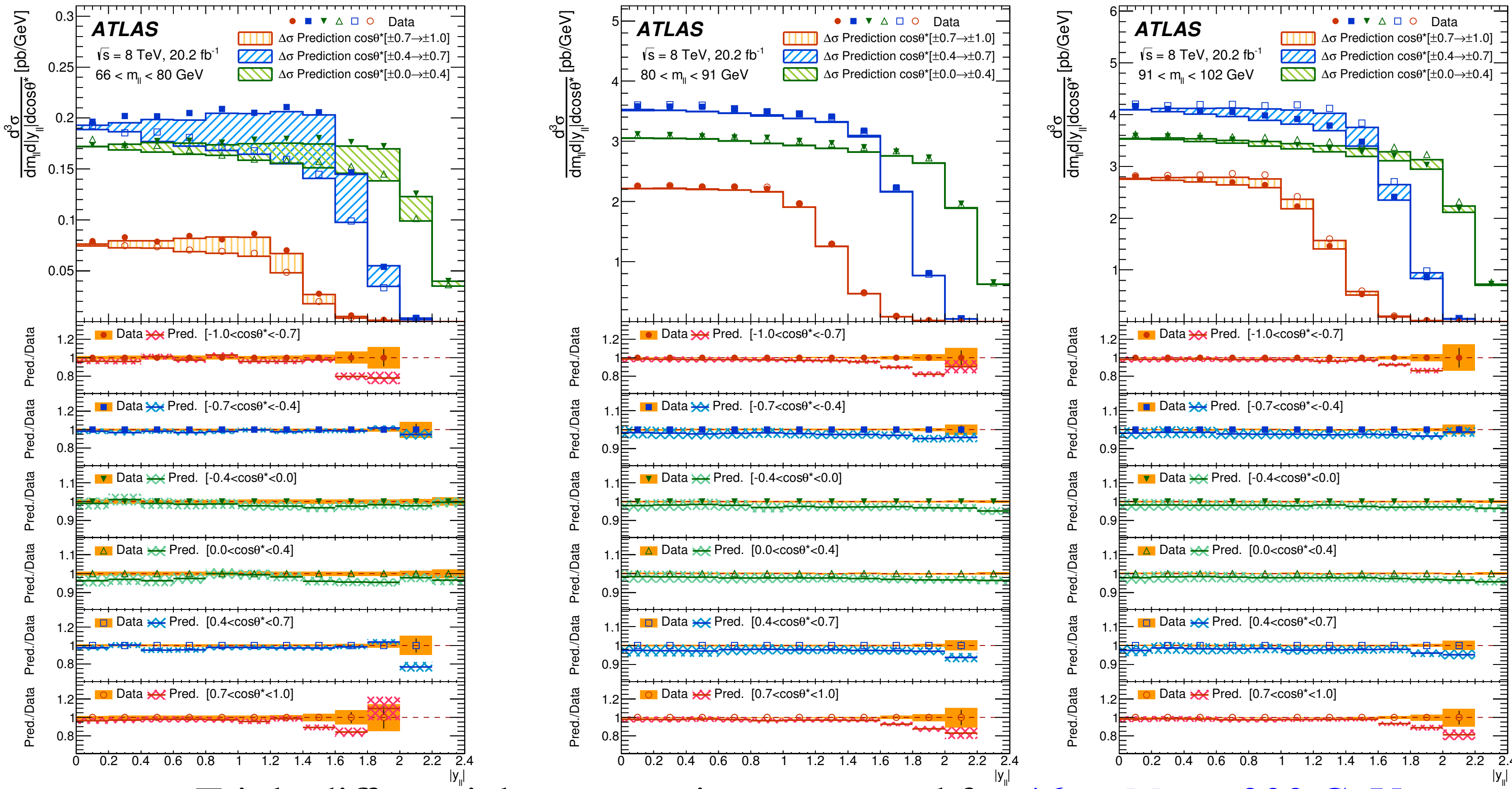

- Triple differential cross section, measured for $46 < M_{\ell\ell} < 200$ GeV range, for CC and CF topology.
- Simultaneous sensitivity to PDFs and $\sin^2\theta_W$, care needed for pure PDF interpretation.

JHEP 12 (2017) 059

Acceptance for Z3D

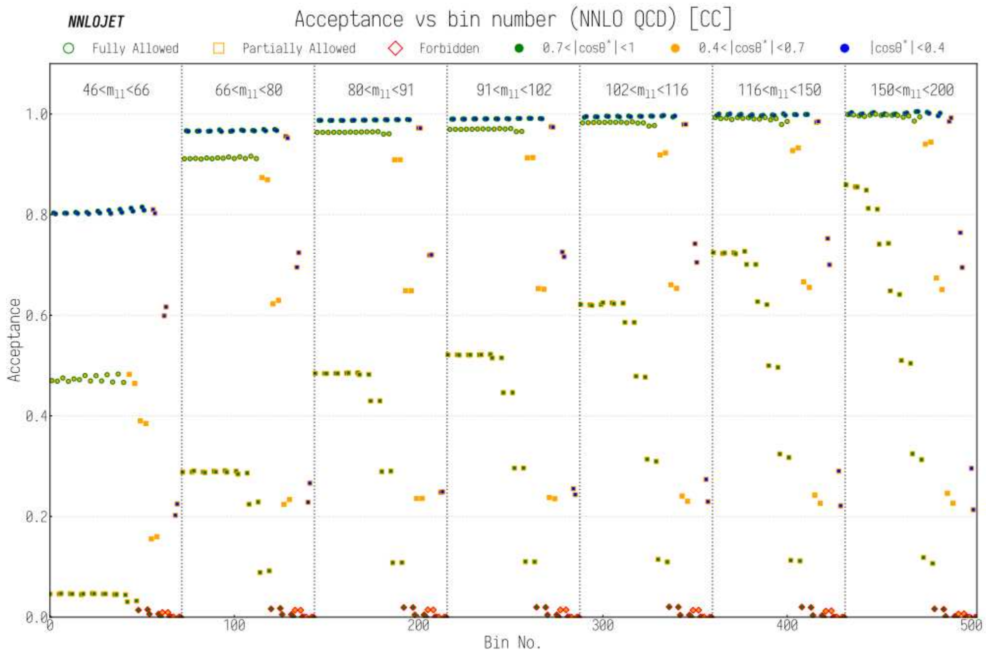

- Acceptance, $A = \sigma_{fid}/\sigma_{tot}$ calculated using NNLOjet program at NNLO ($n_{jet} = 0$) shows strong variation vs $|\cos\theta_{CS}|$, $|y_{\ell\ell}|$ and $M_{\ell\ell}$ ("bin number $= 72i_M + 12i_y + i_{\cos\theta^*}$).
- More than 50% of bins at low $|\cos\theta^*|$ and $M_{\ell\ell} > 66$ GeV have $A > 95\%$.
- Restricting cross section data to these bins (which are also more accurate experimentally) allows to mitigate effect of fiducial cuts.
- Other bins can be converted to FBA.

D. Walker, PhD thesis

MSHT20 fit to ATLAS 8 TeV Z data

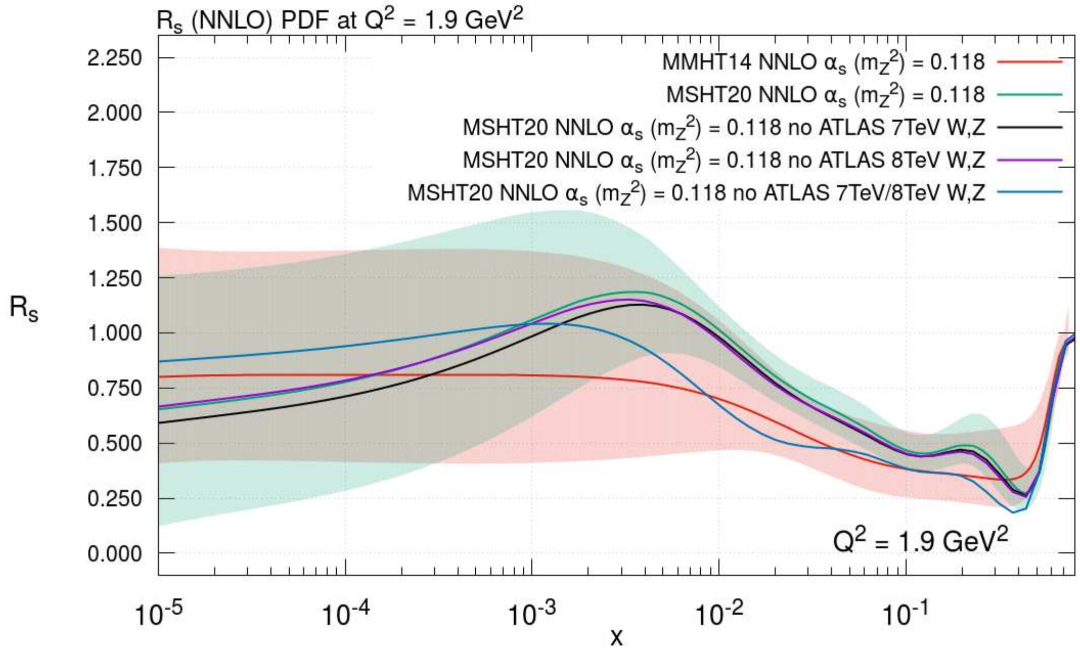

- Default fit is restricted to bins with acceptance $> 95\%$, integrates in $\cos\theta$ to remove $\sin^2\theta_W$ sensitivity.
- Acceptable $\chi^2/dof = 85.6/59$. When the low acceptance bins are included, fit quality is reduced significantly with $\chi^2/dof = 2.1$ without improvement in PDFs (data errors are large for the low acceptance bins).
- The value of $R_s = \frac{s+\bar{s}}{\bar{u}+\bar{d}}$ for $x \sim 0.02$ is driven in the fit by the ATLAS data, keeping 7 or 8 TeV yields similar value, removing both sets lowers R_S to the central result of MMHT14 fit.

arXiv:2012.04684

Z-boson polarization

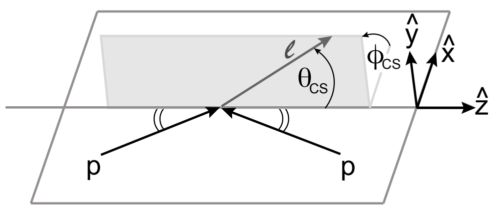

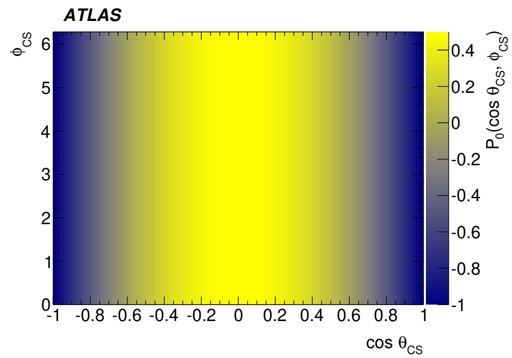

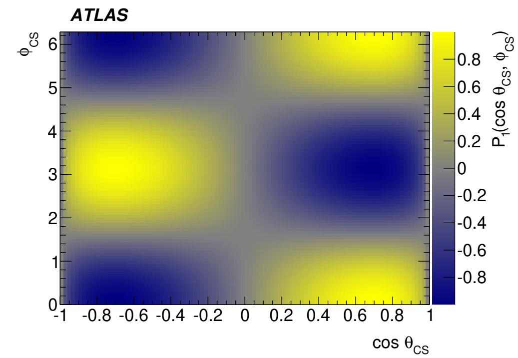

$$\frac{d\sigma}{d\cos\theta d\phi} = (1+\cos^2\theta) + A_0\frac{1}{2}(1-3\cos^2\theta) + A_1\sin 2\theta + \frac{1}{2}A_2\sin^2\theta\cos 2\phi + A_3\sin\theta\cos\phi$$
$$+A_4\cos\theta + A_5\sin^2\theta\sin 2\phi + A_6\sin 2\theta\sin\phi + A_7\sin\theta\sin\phi\,.$$

- W, Z bosons are vector particles and are produced polarized. Decay distributions can be described by spherical harmonics with eight parameters.
- At leading order QCD, only A_4, corresponding to forward-backward asymmetry is present
- At NLO, due to new gq and $g\bar{q}$ diagrams, $A_0 - A_4$ are not zero.
- All coefficients are not zero at NNLO.

Z polarization results

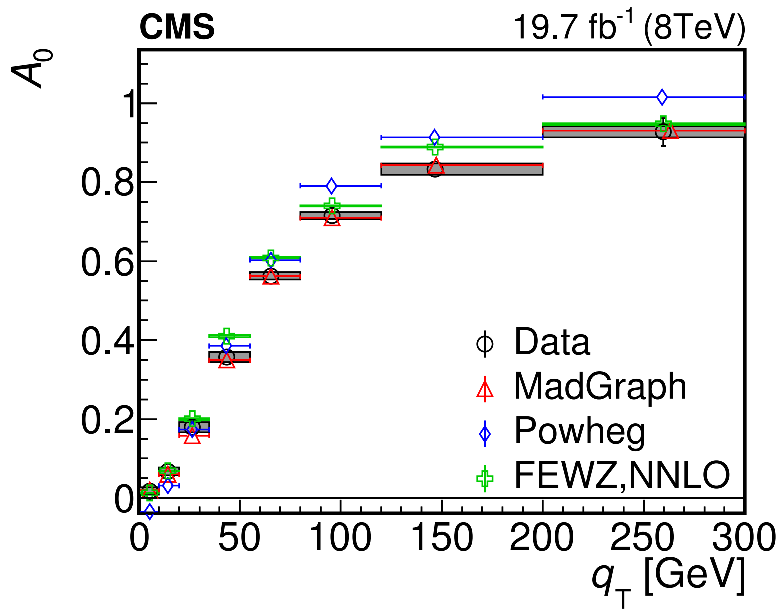

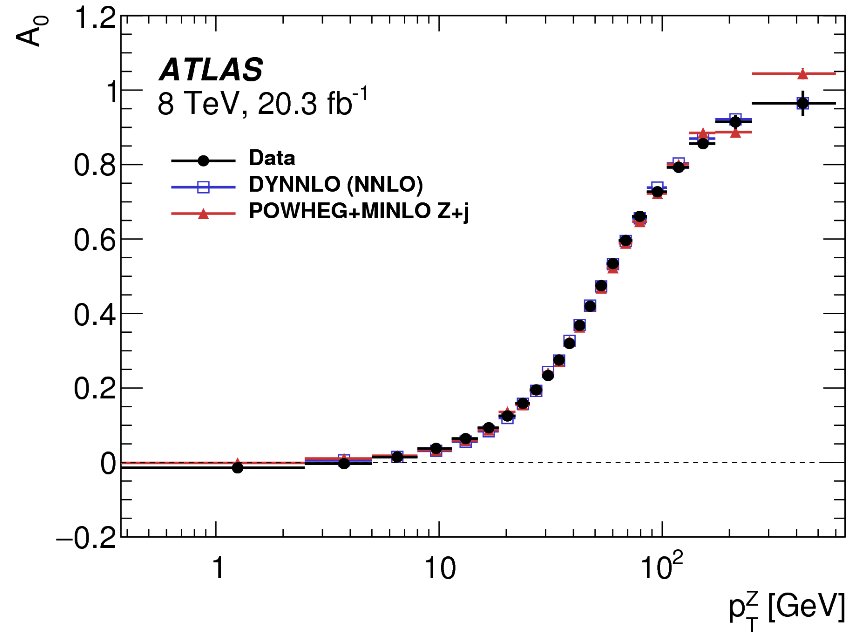

- Measurement of Z polarization coefficients from ATLAS and CMS.
- ATLAS measures all $A_0 - A_8$ polynomials using data from both electron and muon channel and their combination.
- Excellent agreement for A_0 with NNLO QCD.
  CMS, PLB 750 (2015) 154, ATLAS JHEP 08 (2016) 159.

Z angular coefficients

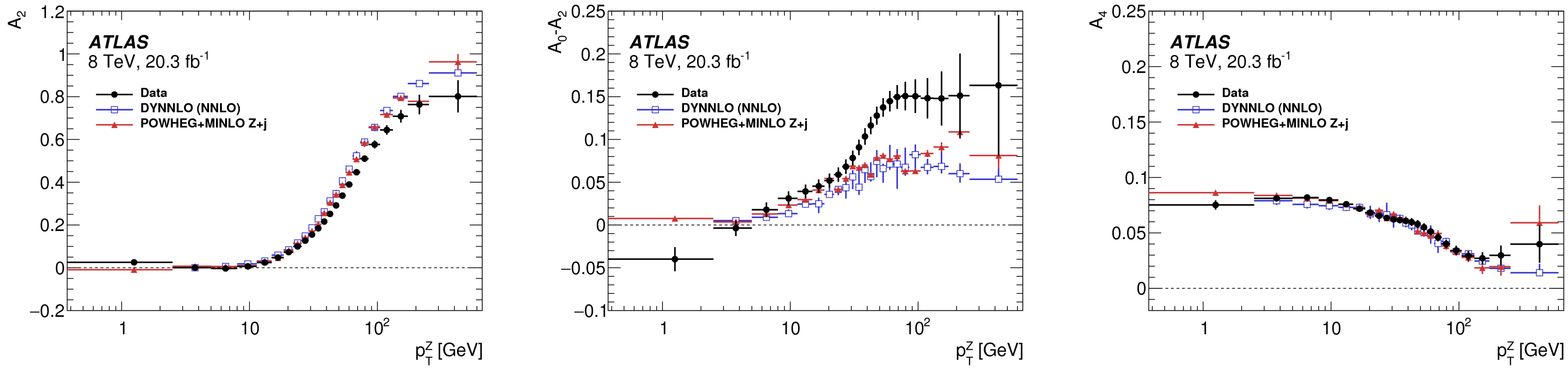

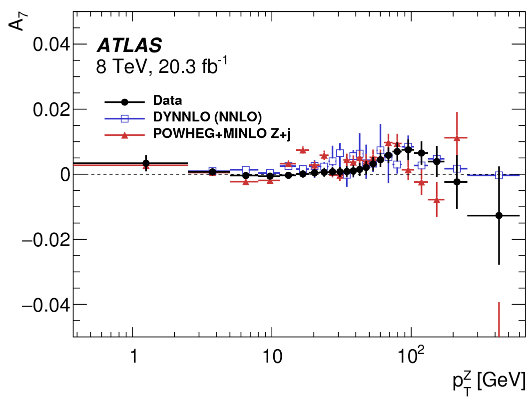

- $A_0 - A_0$ is expected to become non-zero at NNLO, data confirms that
- Data deviates from NNLO expectations for A_2 (and $A_0 - A_2$) at high p_T.
- A_4 measures forward-backward asymmetry, can be used to extract $\sin^2\theta_W$
- Higher order coefficients appear from NNLO, evidence of them in data.

ATLAS JHEP 08 (2016) 159.

A_0 pseudodata profiling and Higgs cross section.

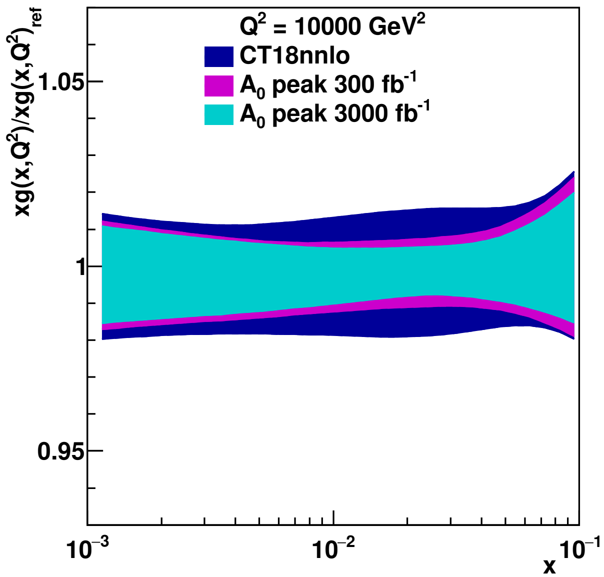

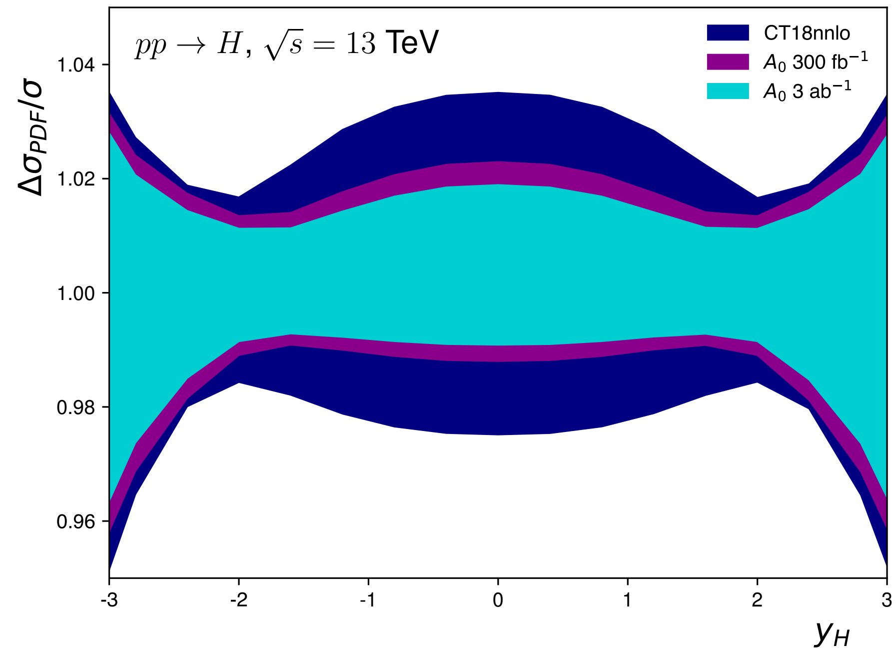

- Studies of A_0 coeffient measured by ATLAS using $\sqrt{s} = 8$ TeV data sample show good compatibility with modern PDF sets for NLO predictions, with $\chi^2/dof = 59/53$ for CT18NNLO set.
- Considering statistical uncertainty plus simplified systematics, pseudodata for $\mathcal{L} = 300, 3000\ \mathrm{fb}^{-1}$ are profilied using `xFitter`.
- $\rightarrow$ significant reduction of gluon uncertainty, leading to visible reduction in PDF uncertainty for $gg \rightarrow H$ process, computed using MCFM.

Measurement of Z_{p_T}

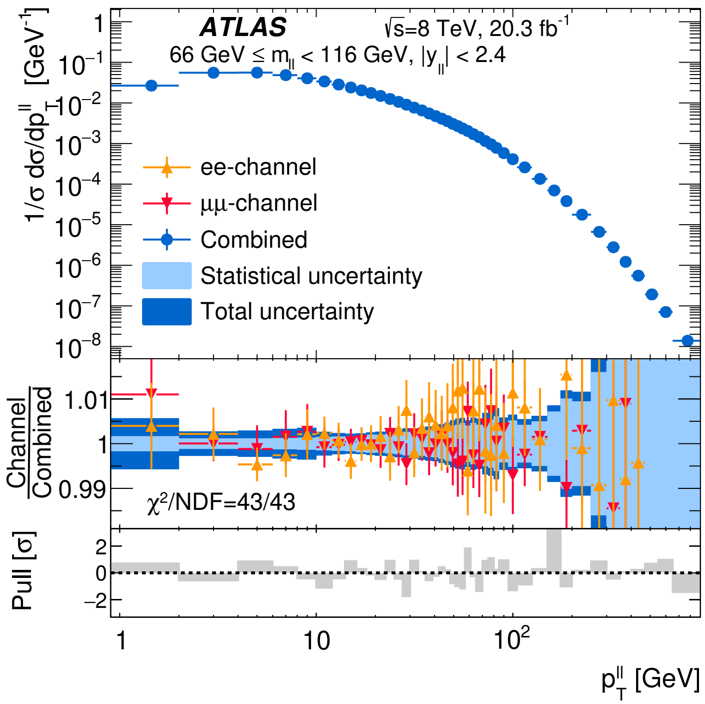

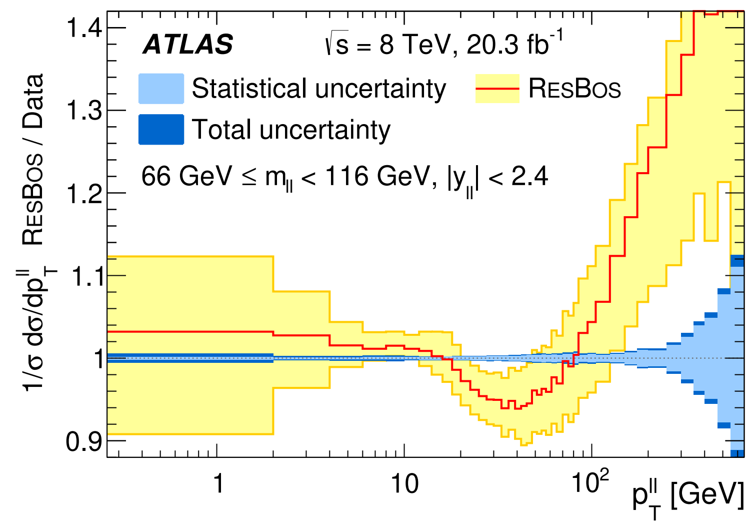

- Several measurements of Z_{p_T} at $\sqrt{s} = 7, 8, 13$ TeV by ATLAS and CMS.
- ATLAS measurements use both $Z \to ee$ and $Z \to \mu\mu$ channels, which have comparable accuracy. The combined result is accurate to better than 0.5% for $P_T < 100$ GeV range.
- Data can be used to fit theory parameters to propagate their impact to W mass analysis. Must be done coherently with PDF uncertainties.

ATLAS, arXiv:1512.02192

Describing Z_{p_T} distribution

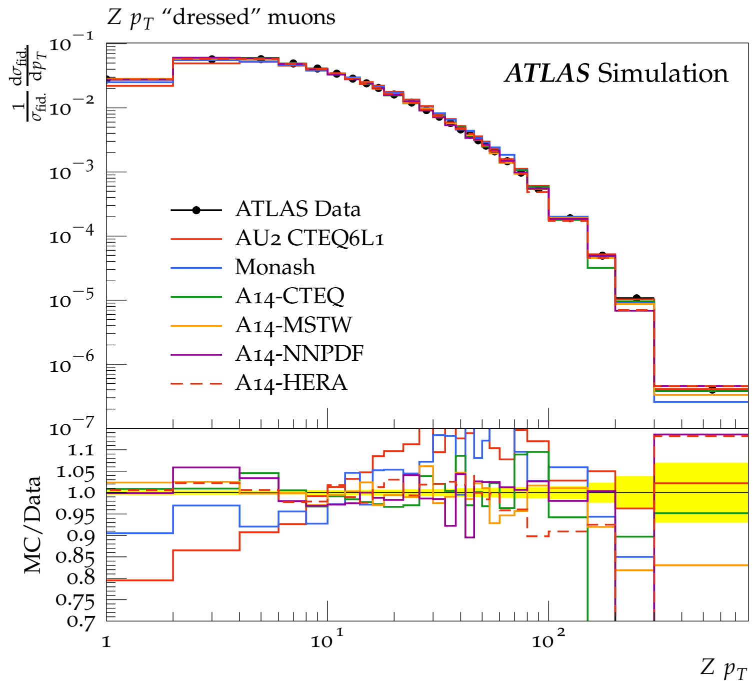

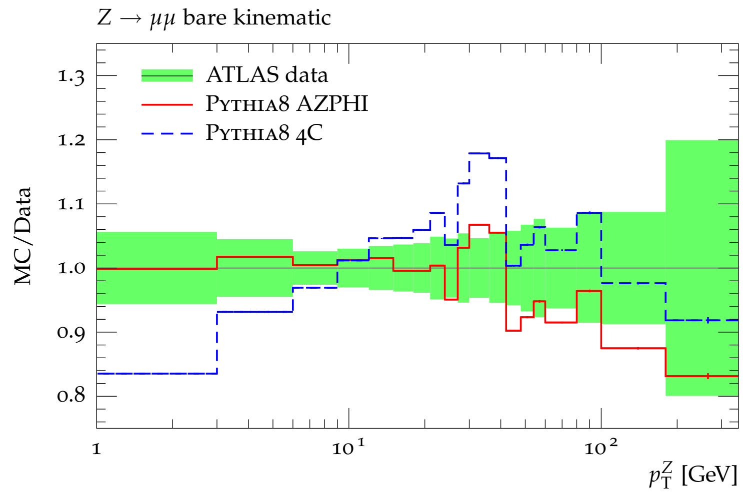

- Pythia tunes to "global" data (left) or restricted to Z_{p_T}
- Dedicated tunes can describe the data very well with just few tuning parameters (primodial k_T, ISR $\alpha_S(M_Z)$ and ISR p_T cut-off)

ATL-PHYS-PUB-2014-021, ATL-PHYS-PUB-2013-017

Measurements of W+c

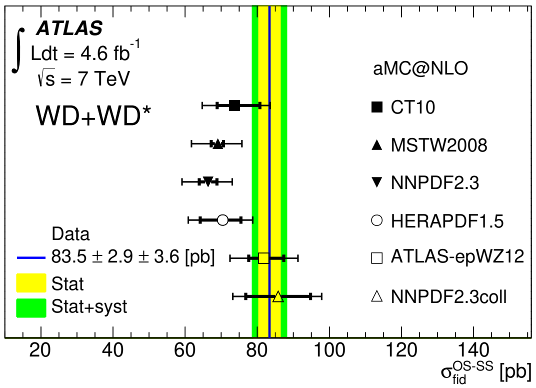

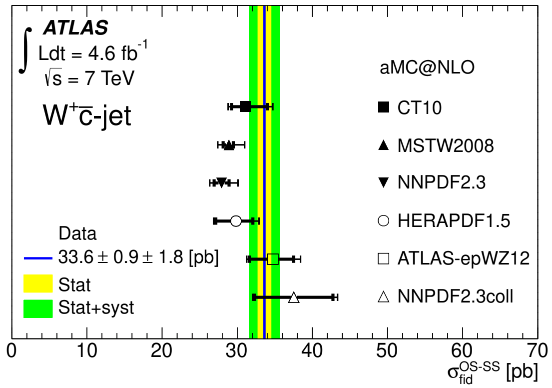

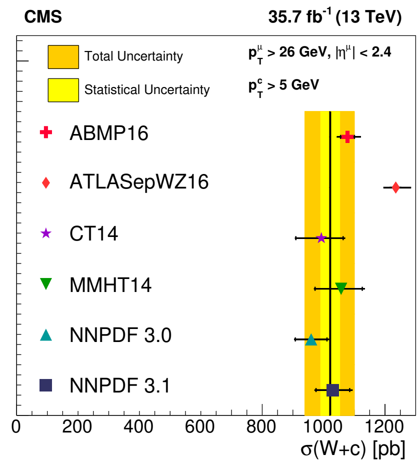

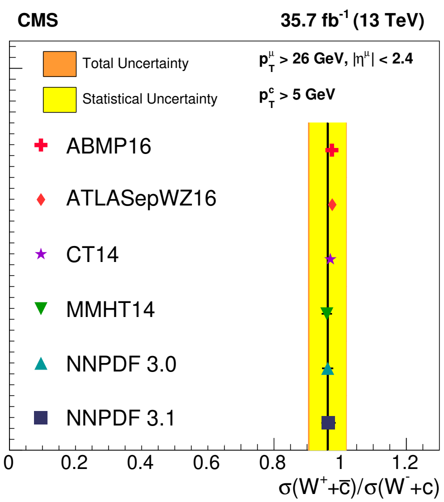

- Measurements of $\sigma(W^\pm c^\mp) - \sigma(W^\pm c^\pm)$ from ATLAS using c-jets tagged by soft muons and $D^{(*)}$ mesons, to probe strange-sea PDF using $gs \to Wc$ process.
- W^+ vs W^- data can be used to constrain $s/\bar{s}$
- NLO scale uncertainties are larger than data uncertainties even for this $\sqrt{s} = 7$ TeV result: need for NNLO analysis.

ATLAS: JHEP 02 (2014) 013, CMS: EPJC 79 (2019) 269

NNLO corrections for $W + c$

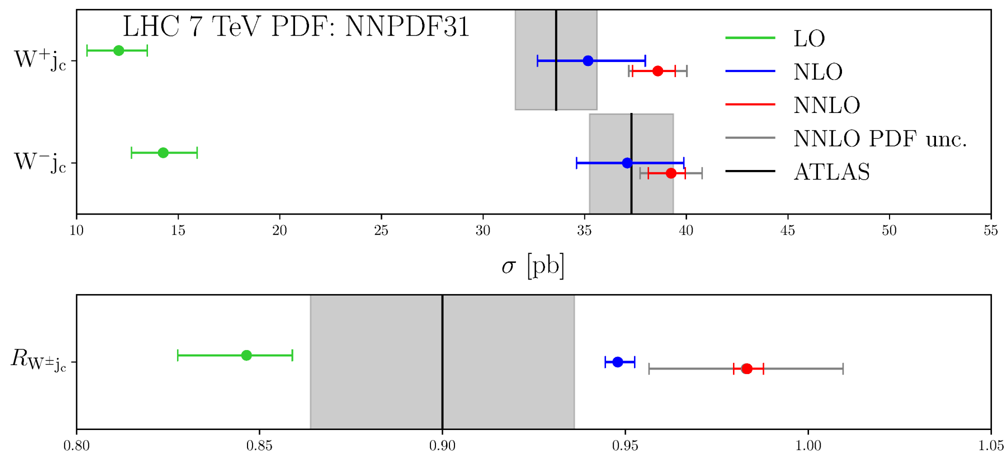

- Recent calculations of NNLO corrections for $W + c$ jet process.
- Corrections are significant, uncertainties are reduced significantly too.
- However mis-match between flavour k_T and anti-k_T algorithms used for reconstruction
- Measurements of $W + D^{(*)}$ production are more accurate vs $W + c$ jet: predictions including charm fragmentation would be highly welcome.

arXiv:2011.01011

$\gamma - Z$ interference measurement and PDF constraints

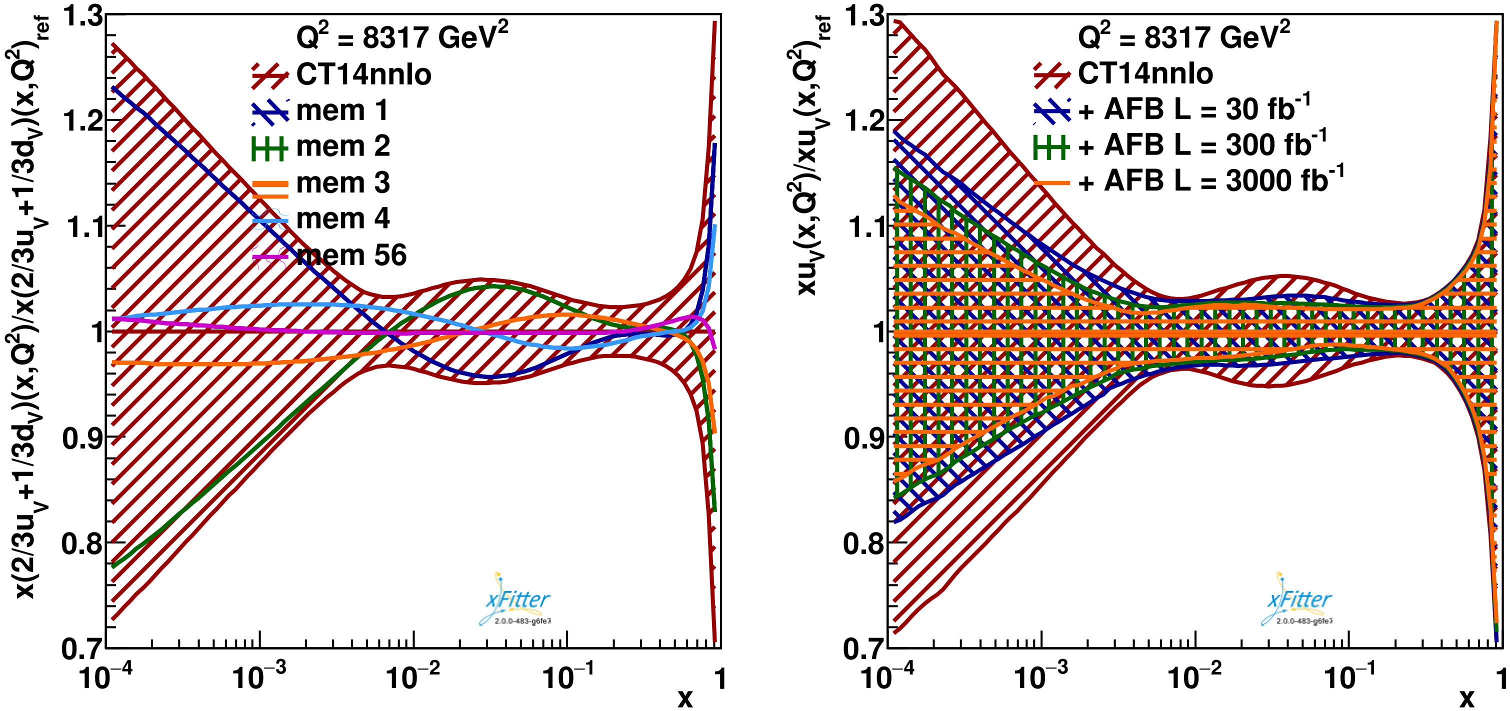

- Off-resonance FB asymmetry ("A_4")is sensitive to $\gamma^* Z$ interference, proportional to $\frac{2}{3}u_V(x, Q^2) + \frac{1}{3}d_V(x, Q^2)$
- Can be used to constrain this linear combination of PDFs, however other observables are needed to decompose separate u_V and d_V contributions.

xFitter, JHEP 1910 (2019) 176

$W^{\pm} \to \ell^{\pm}\nu$ charge asymmetry measurement

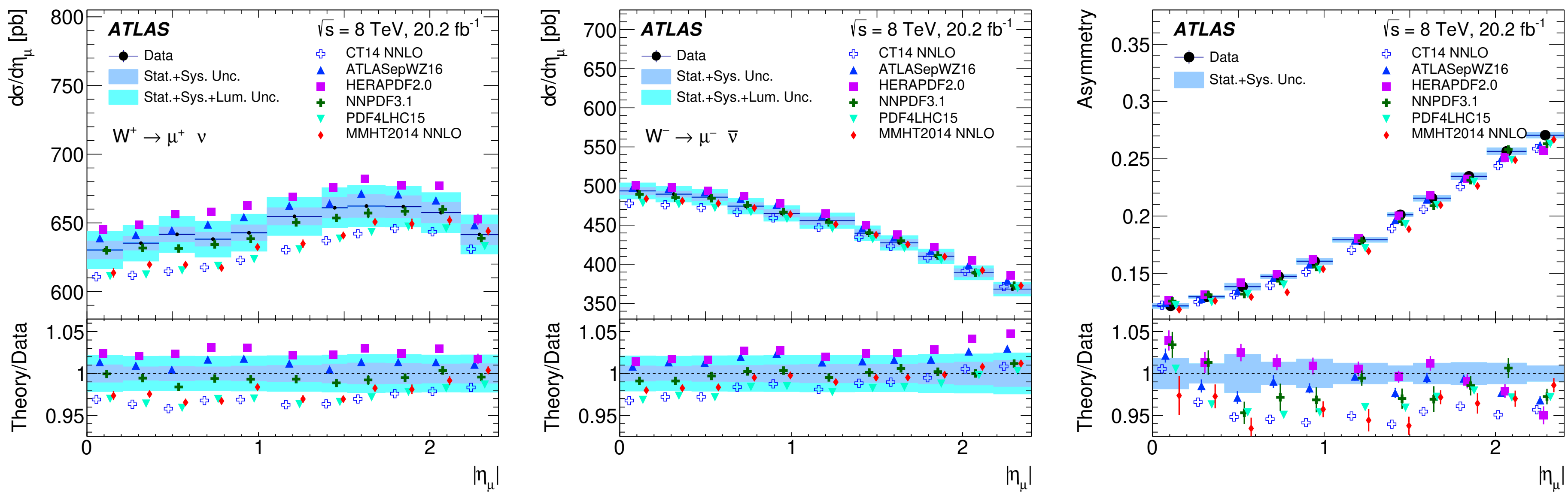

- W lepton charge asymmetry is at leading order proportional to $u_V - d_V$.
- Data accuracy is limited by systematic uncertainties, driven by pileup (lepton fakes, E_T^{miss} reconstruction). Could be measured better in dedicated low pileup samples.
- Data agree better with PDFs including ATLAS 7 TeV measurement (and HERAPDF2.0).

ATLAS, EPJC 79 (2019) 760

Main experimental techniques to measure M_W

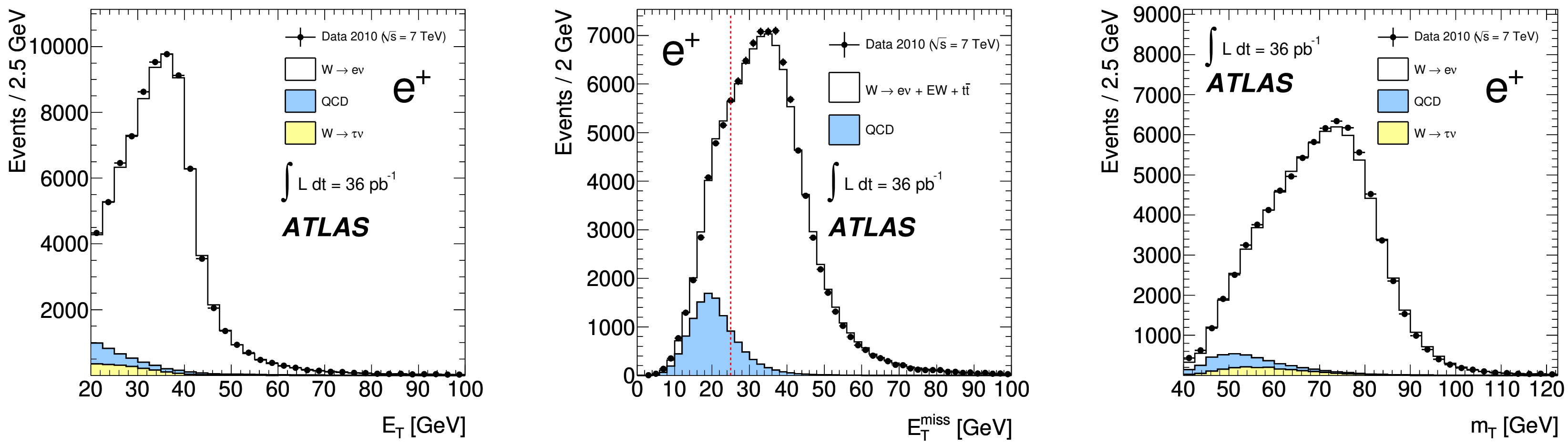

$$pp \to X + W^{\pm}, \quad W^{\pm} \to \ell^{\pm}\nu$$

- Fit lepton ($e^{\pm}$ and $\mu^{\pm}$) p_T distribution around Jakobian peak. Most accurate experimentally, robust to pileup, most prone to W p_T modeling problems.
- Fit missing energy distribution E_T^{miss}. Requires modeling of hadron recoil. Hard in case of large pileup.
- Fit transverse mass M_T. Needs good E_T^{miss} reconstruction. Least prone to modeling issues.

Fits can be performed using binned in η-lepton, which can be useful to control PDF effects.

Theory inputs for W production modeling

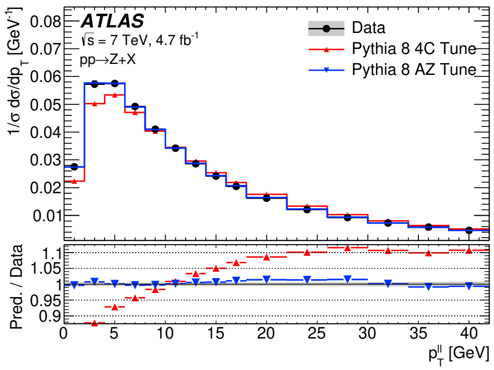

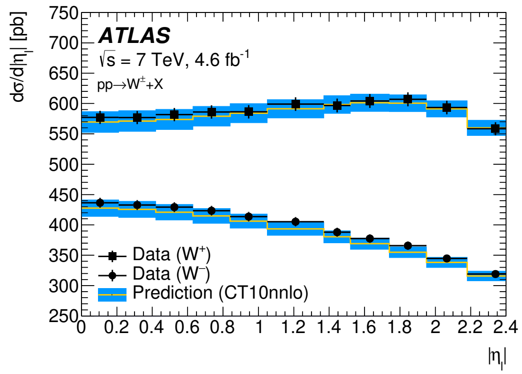

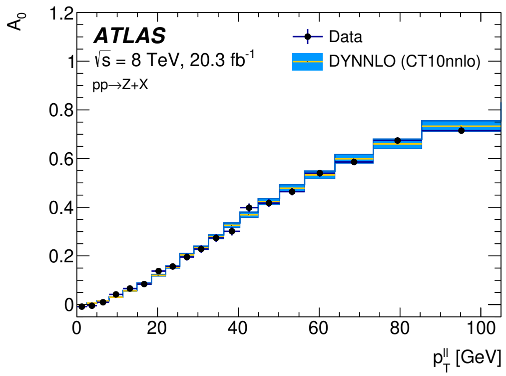

- Control over modeling of W production is essential for accurate W-boson mass measurement.
- Use data-driven methods as much as possible.
- Control W_{p_T} using measurements of Z_{p_T}. W_{p_T} can be measured directly → dedicated low pileup runs in 2017 at 5 TeV and 13 TeV.
- W rapidity is probed using lepton η distribution. Perform measurement in slices of η.
- W polarization can be checked by the Z polarization measurements.

m_W results

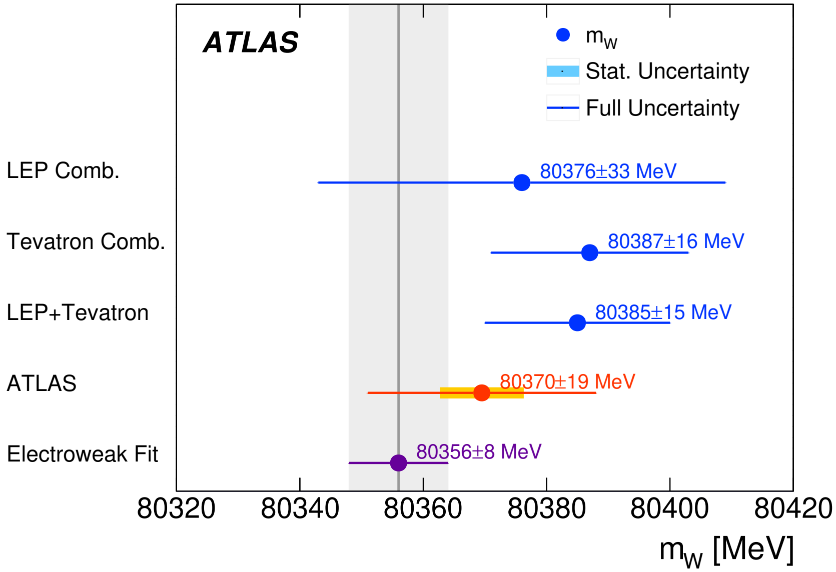

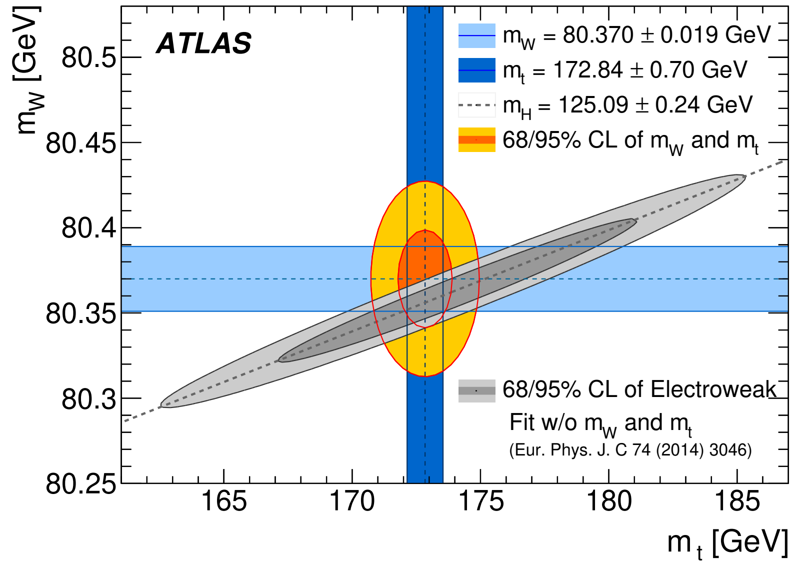

- Measurement accuracy is better than combined LEP, comparable to Tevatron individual best measurements.
- Modeling uncertainties dominate, but they can be reduced using additional measurements.
- ATLAS data are in perfect agreement with the expectations from the electroweak fit.

EPJ C78 (2018) 110

Top quark mass measurements

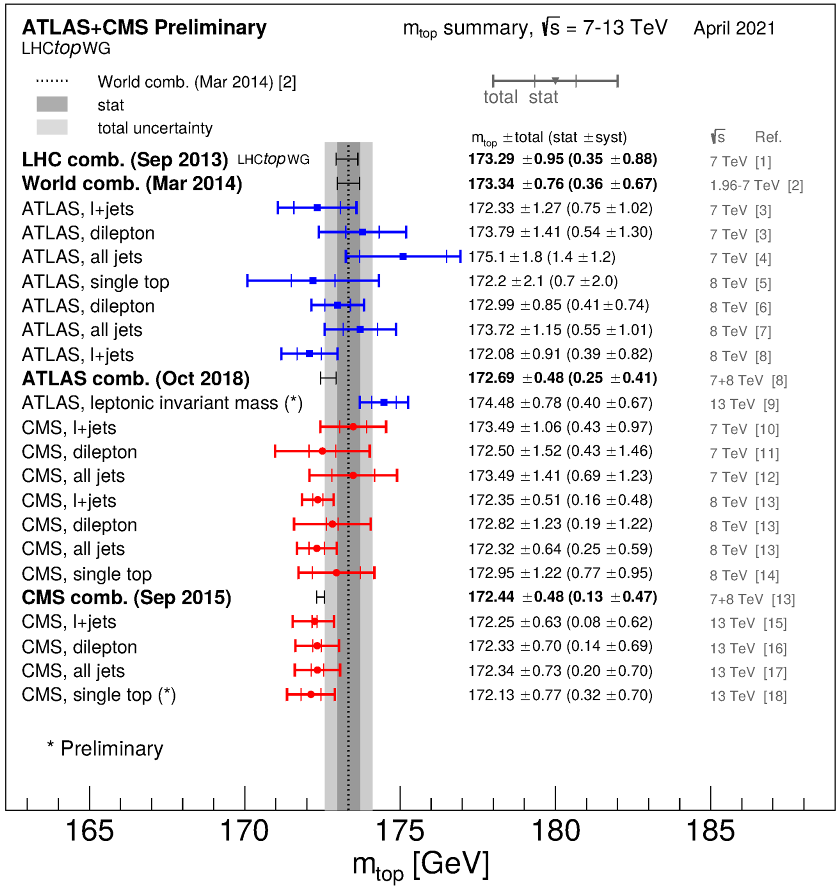

- Direct methods to estimate m_t become systematics limited, with additional interpretation uncertainties
- Methods based on $\sigma_{t\bar{t}}$ depend strongly on PDFs, α_S

$\sigma_{t\bar{t}}$ measurements

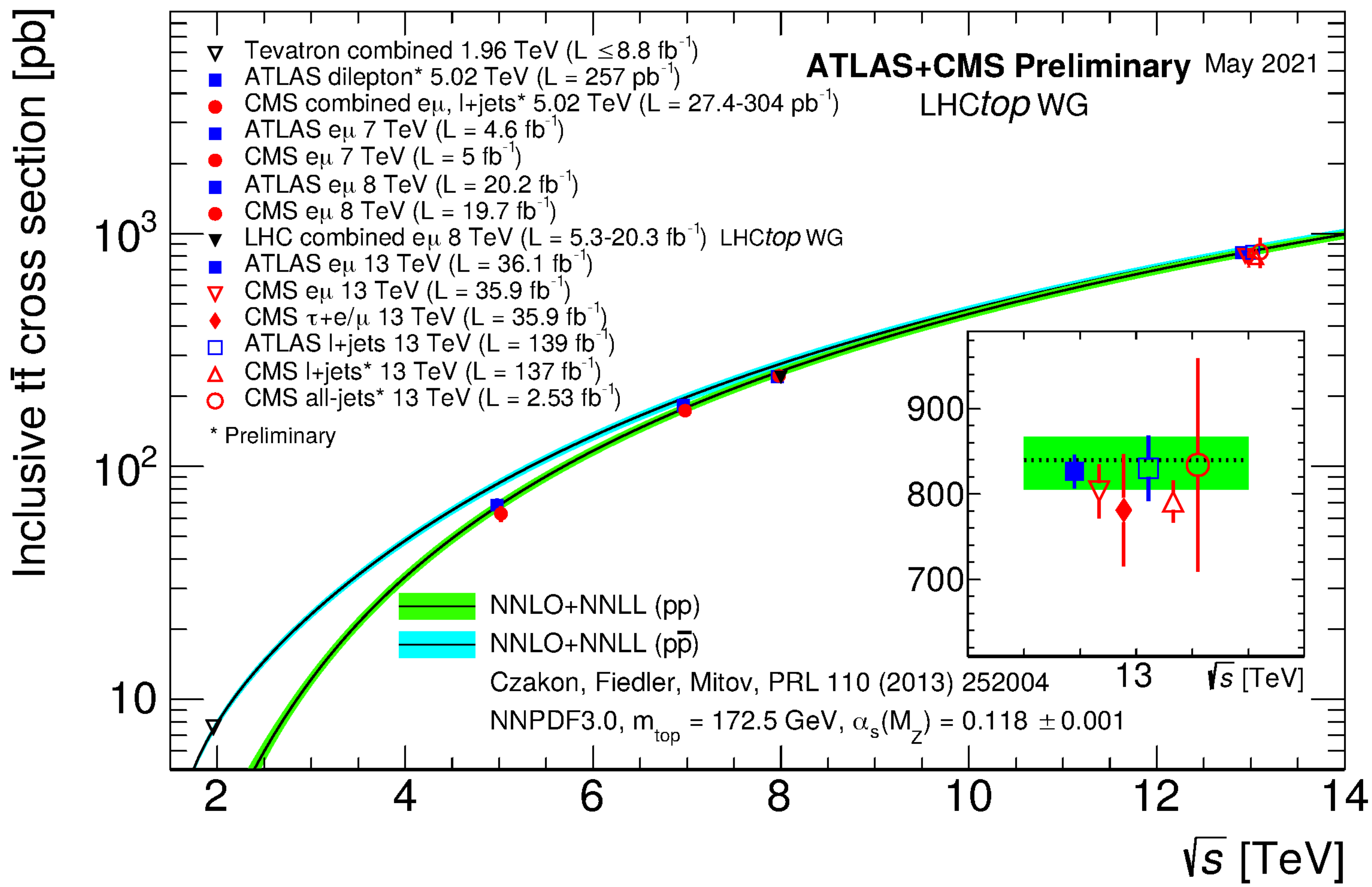

Accurate measurement of the cross section for different $\sqrt{s}$.

$\sigma_{t\bar{t}}/\sigma_Z$ ratio measurement

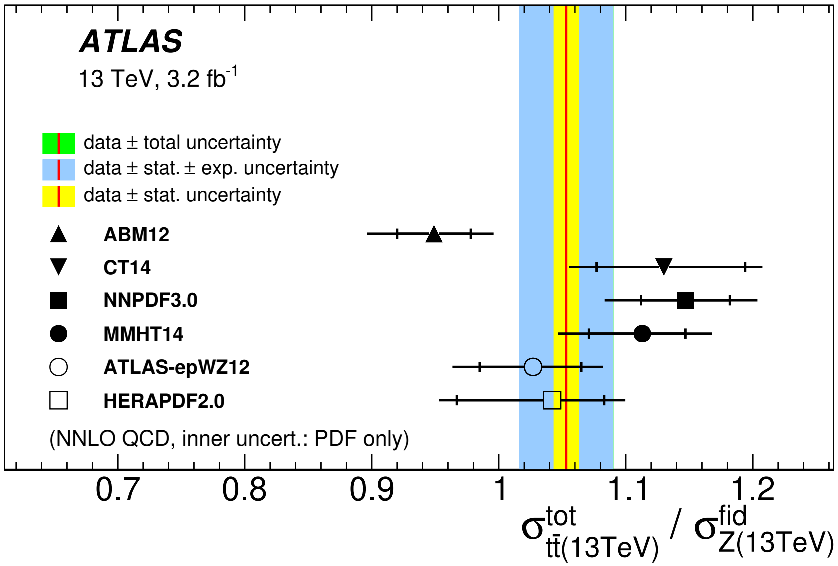

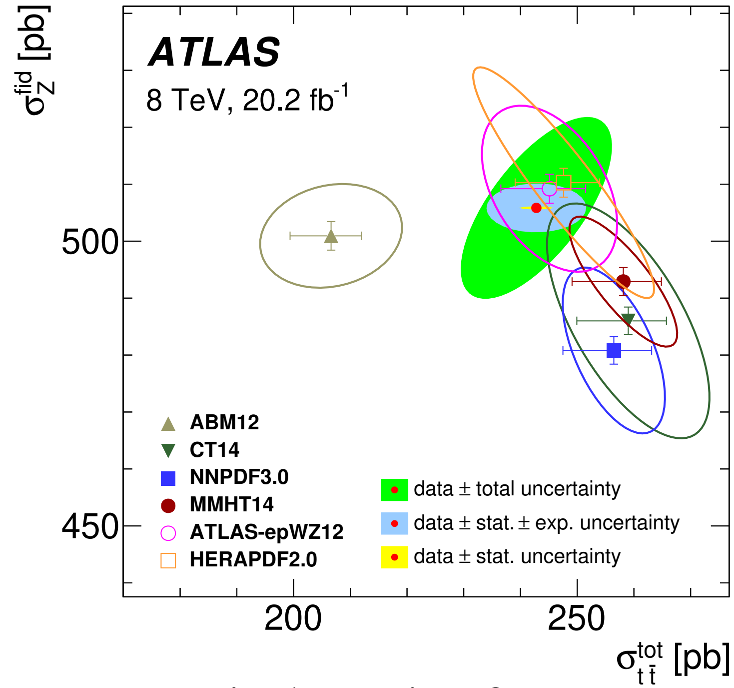

- Production of $t\bar{t}$ and Z dominated by gg and $q\bar{q}$, respectively: ratio of cross sections is sensitive to gluon/sea at $x \sim 0.1$.
- Dedicated measurement of σ_Z^{fid} at $\sqrt{s} = 13$ TeV for

$$\frac{\sigma_{t\bar{t}}^{\text{tot}}}{\sigma_Z^{\text{fid}}} = \frac{2\sigma_{t\bar{t}\to X+e\mu}^{\text{tot}}}{\sigma_{Z\to ee}^{\text{fid}} + \sigma_{Z\to\mu\mu}^{\text{fid}}}$$

- Evaluation of correlations for existing 7, 8 TeV measurements.

ATLAS, JHEP 02 (2017), 117

Correlated Z and $t\bar{t}$ cross sections

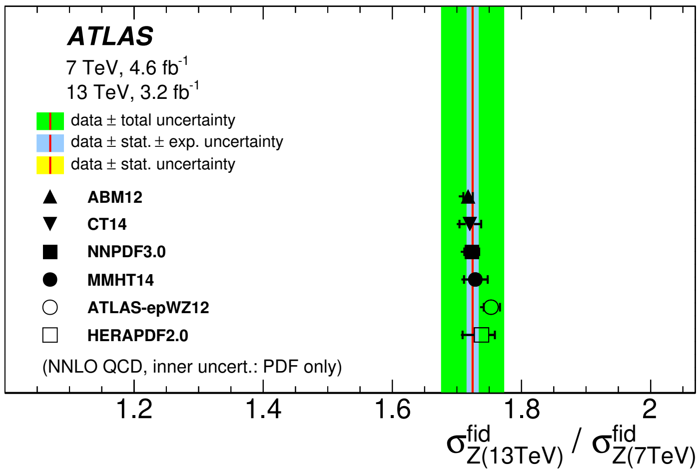

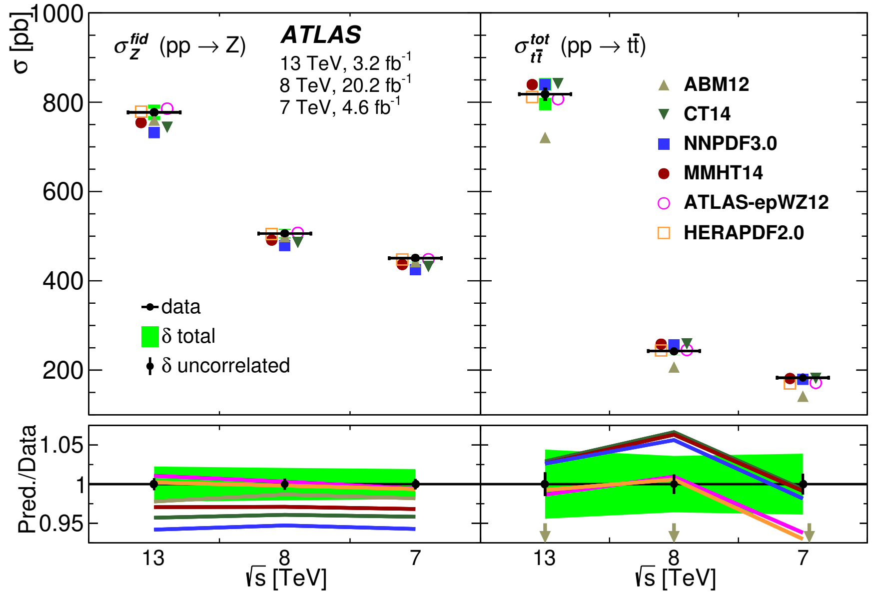

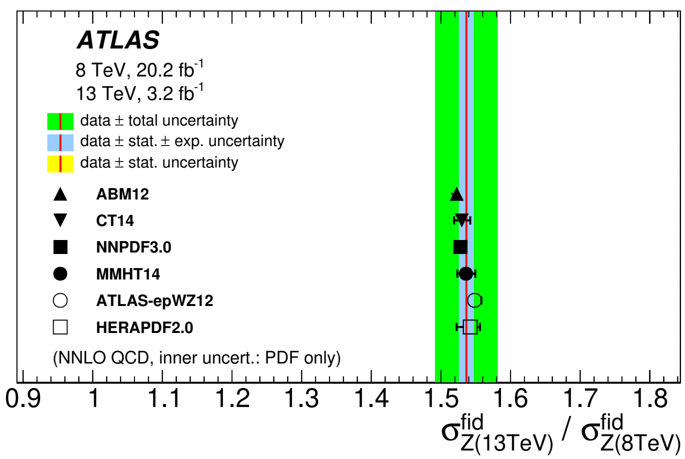

- Ratio of σ_Z^{fid} at different $\sqrt{s}$ has small PDF uncertainty, smaller vs lumi error.
- For σ_Z, data are systematically higher vs predictions of CT14, NNPDF3.0 and MMHT14 PDF sets.

Recap

- Accurate measurements of $\sigma_{t\bar{t}}$ can be used for alternative determination of $m_{t\bar{t}}$ with small theoretical uncertainties.
- Large sensitivity to the gluon distribution and α_S: constrain them from the data.
- Use inclusive jet production, (normalized) differential $t\bar{t}$ production.

Inclusive jet measurement at 13 TeV

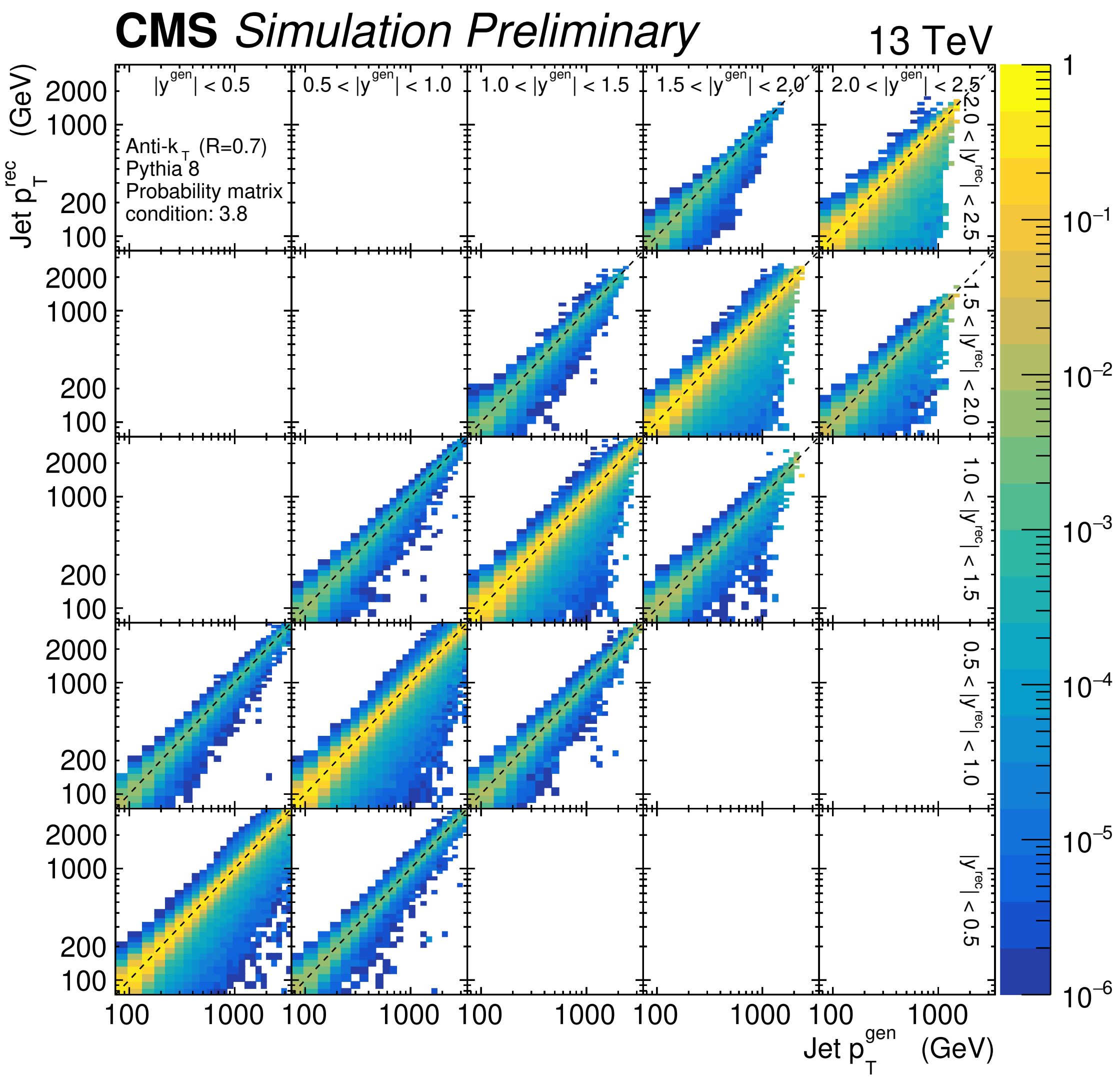

Transfer matrix for unfolding

CMS PAS-20-011

- Measurement with jet radia $R = 0.4(0.7)$, double differential in p_T and y.
- Triggers with thresholds from $\sim$ 75 GeV, different prescale factors, no prescale above $\sim$ 600 GeV
- CMS particle flow jet reconstruction.

Correlation matrix for $R = 0.7$

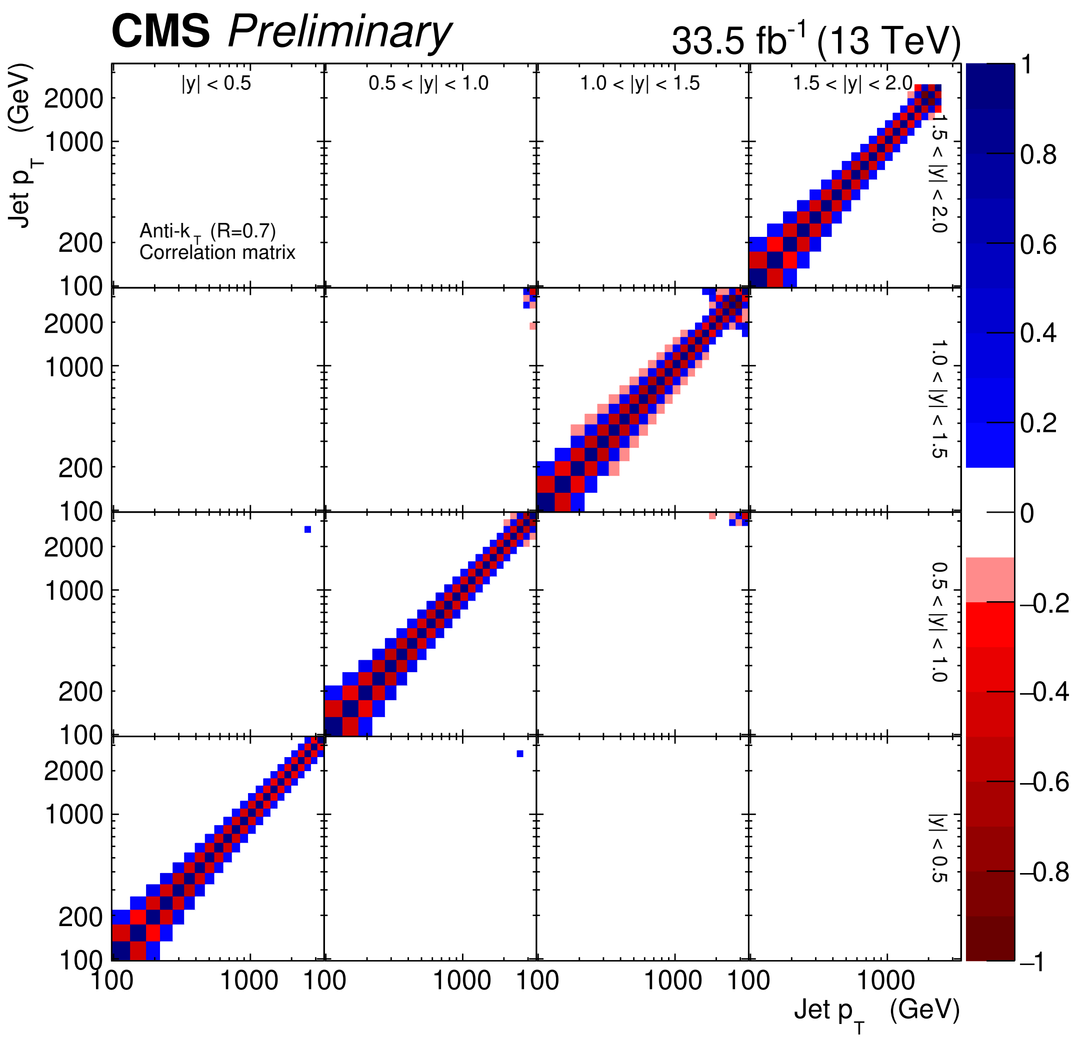

Correlation matrix

Unreglarised unfolding using TUnfold:

$$\chi^2 = \min_x (Ax - y - b)^T V^{-1} (Ax - y - b)\,.$$

Here y, b stand for the detector level measurement, and unmatched background. V is covariance matrix at detector level. Typical correlation pattern, with anti-correlation for neighbouring bins.

Measurement uncertainties

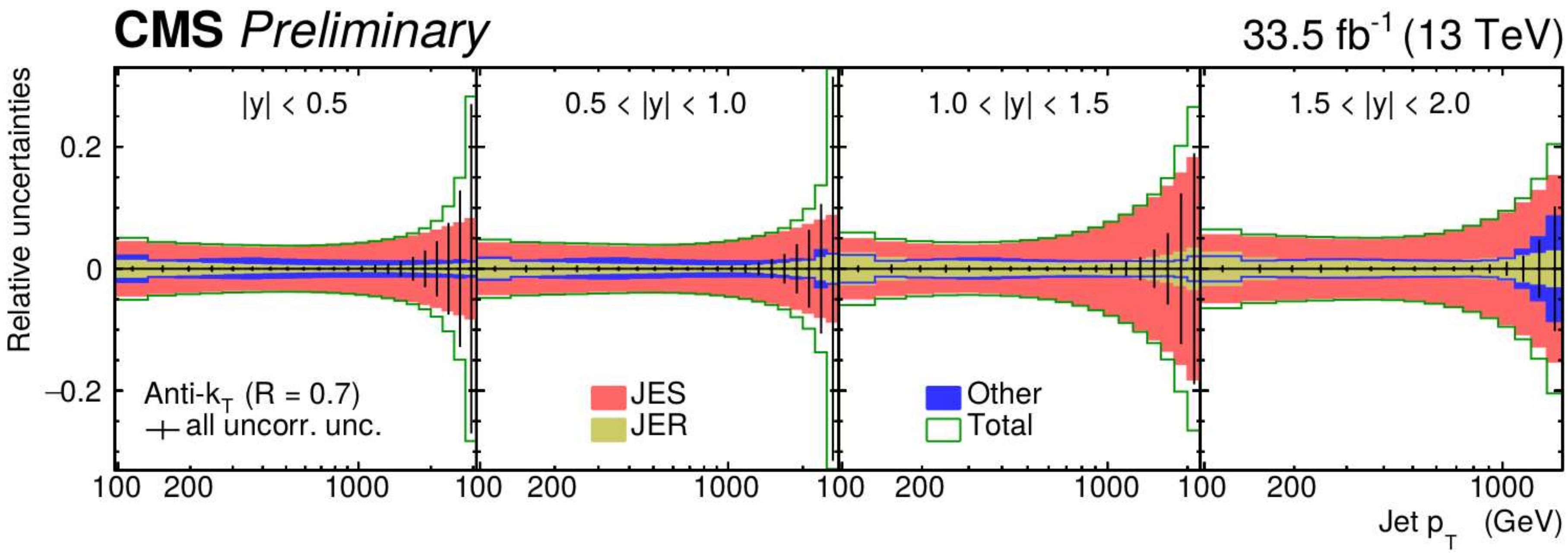

- Largest uncertainties from jet energy scale and resolution.
- Visible uncertainty from luminosity, modelling of the transfer matrix (“Other”).
- Statistical uncertainties are sizable at high p_T only.

→ correct treatment of correlations due to systematic uncertainties are crutial for interpretation of the data.

Theoretical predictions

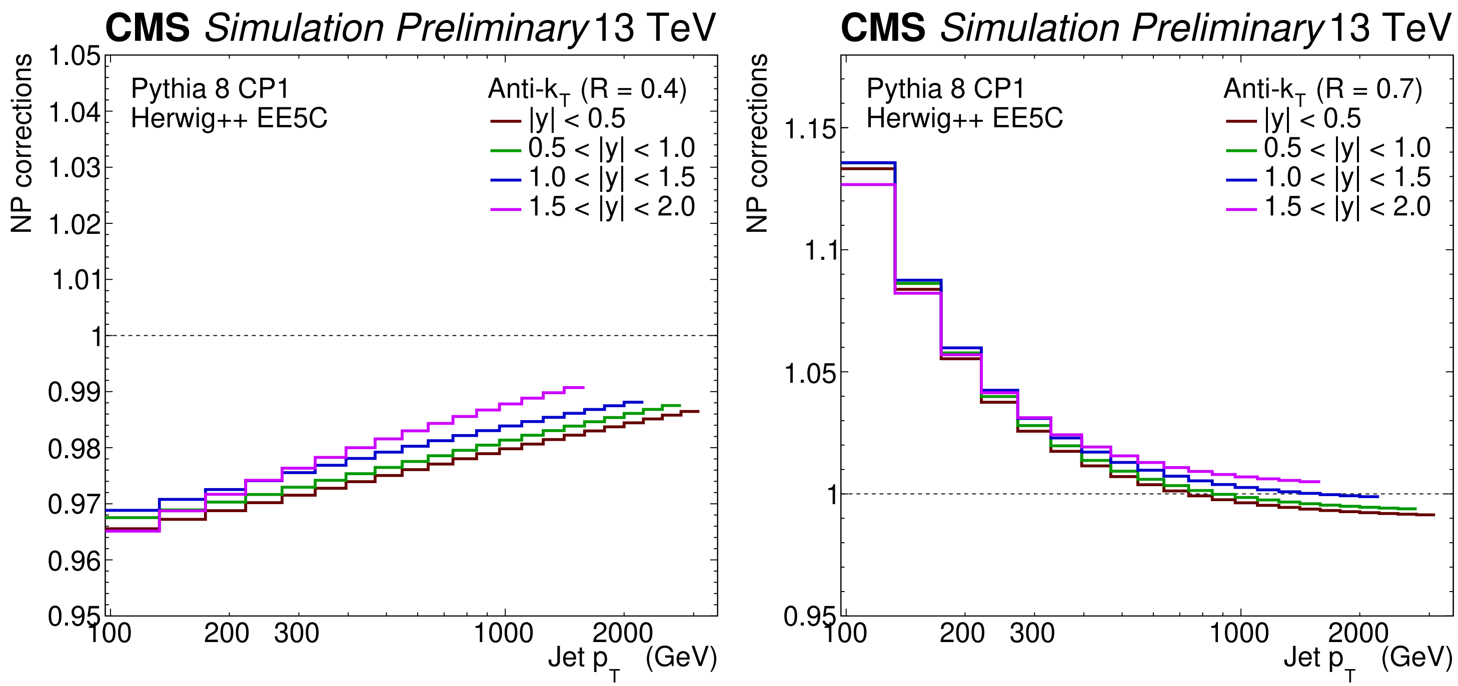

- Fixed order QCD predictions at NLO and NNLO using NNLOJET implemented in FastNLO. NLO+NLL predictions with jet radius and threshold resummation. NLO electroweak corrections
- Non-perturbative corrections from Pythia with MPI/hadronisation over without. Negative for $R = 0.4$, positive for $R = 0.7$.

Data to theory comparison

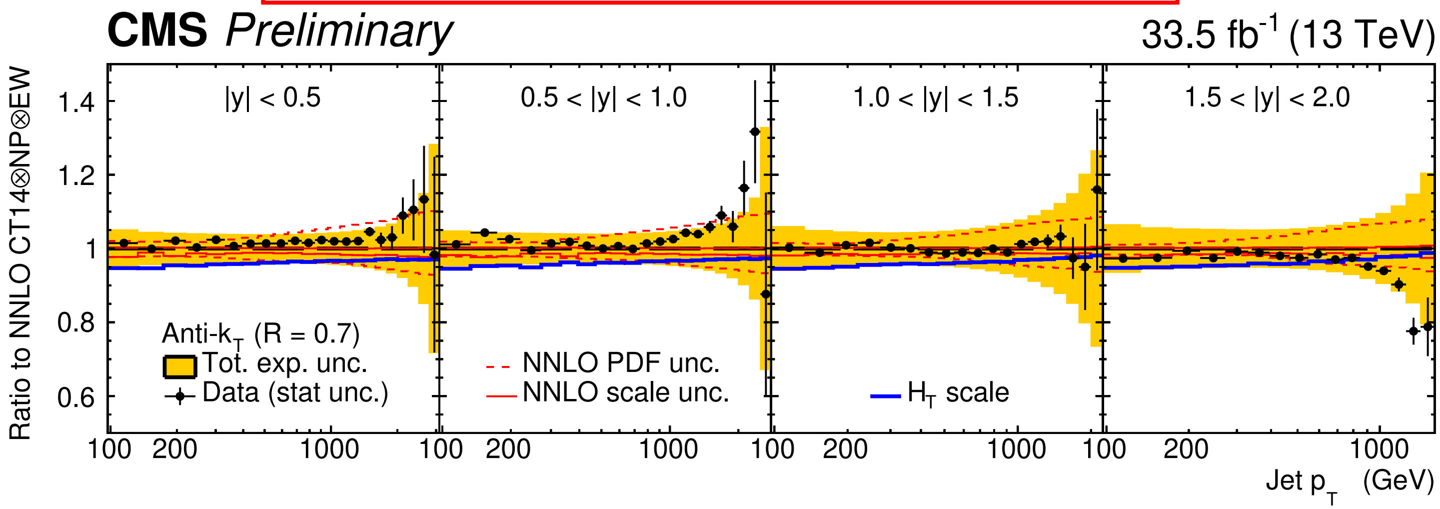

- Reasonable agreement between data with $R = 0.7$ and NNLO theoretical predictions using CT14 PDF set → use these data for following analysis
- QCD analysis performed using xFitter:
  - PDF profiling, using CT14 PDF set as input
  - Full PDF fit to HERA, CMS jet and differential $t\bar{t}$ data
  - Also including SMEFT (dimension 6 operators), for unbiased BSM study.

PDF fit vs PDF profiling

In the fit, PDFs (and other variables of interested, e.g. $\alpha_S(M_Z)$) are parameterised at the starting scale using parameters α, evolved to other scales, and convoluted to determine predictions $m_i(\alpha)$ for all data points μ_i. The experimental systematic uncertainties Γ_{ij}^{exp} are profiled in the fit:

$$\chi^2(b_j, \alpha) = \sum_i \left(\frac{\mu_i + \sum_j \Gamma_{ij}^{exp} b_j - m_i(\alpha)}{\sigma_i} \right)^2 + \sum_j b_j^2 \,.$$

It is important to have sufficient data sample to constraint PDFs.

In the PDF profiling, PDFs are taken from LHAPDF (already fitted to other data) using eigenvector representation. The profiled log likelihood function is extended to include PDF uncertainties:

$$\chi^2(b_j, b_j^{pdf}) = \sum_i \left(\frac{\mu_i + \sum_j \Gamma_{ij}^{exp} b_j - \left[m_i + \sum_j \Gamma_{ij}^{pdf} b_j^{pdf} \right]}{\sigma_i} \right)^2 + \sum_j b_j^2 + \sum_j (b_j^{pdf})^2 \,.$$

The fitted parameters b_j^{pdf} and their reduced uncertainties, are applied to the PDF eigenvectors, which can be re-diagonalized and produce a new profiled PDF set.

PDF and α_S based on CT14 profiling.

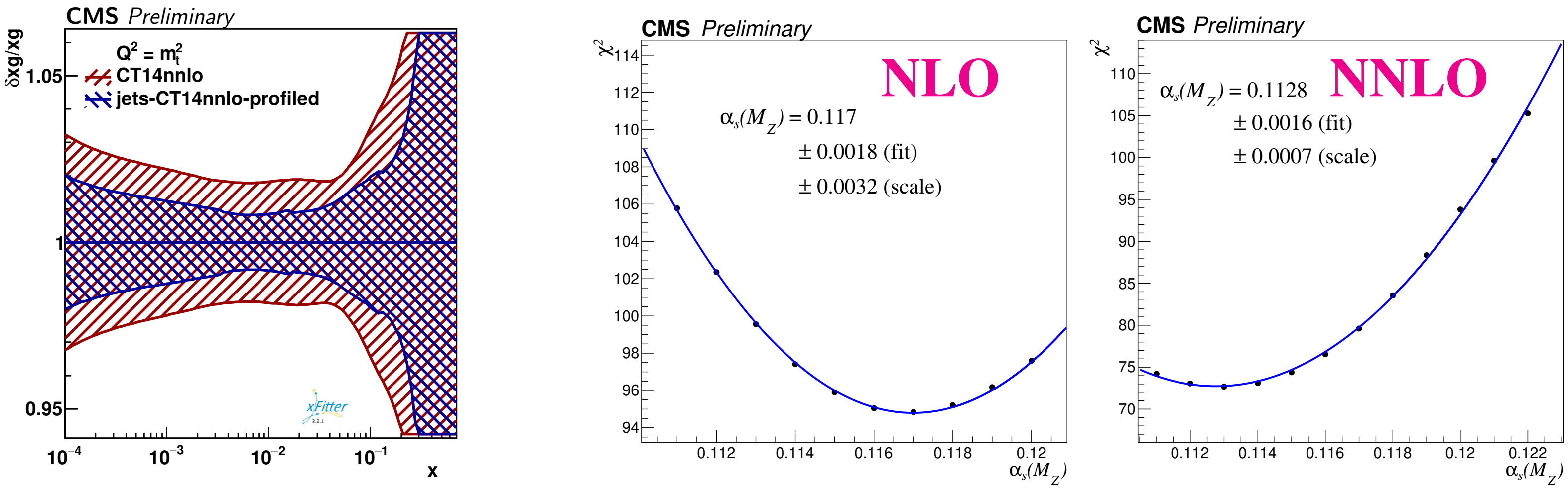

- Significant (potential) reduction of the gluon uncertainty, for both NLO and NNLO fits. Note, however potential increase of the tolerance in the global fit due to tensions between experimental measurements.
- Good fit quality (to 78 data points), which is improved for NNLO.
- α_S scale uncertainty is much reduced for NNLO.
- Central value of α_S is lower at NNLO.

Measurement of $\sigma_{t\bar{t}}$ and extraction PDFs+α_S+m_t

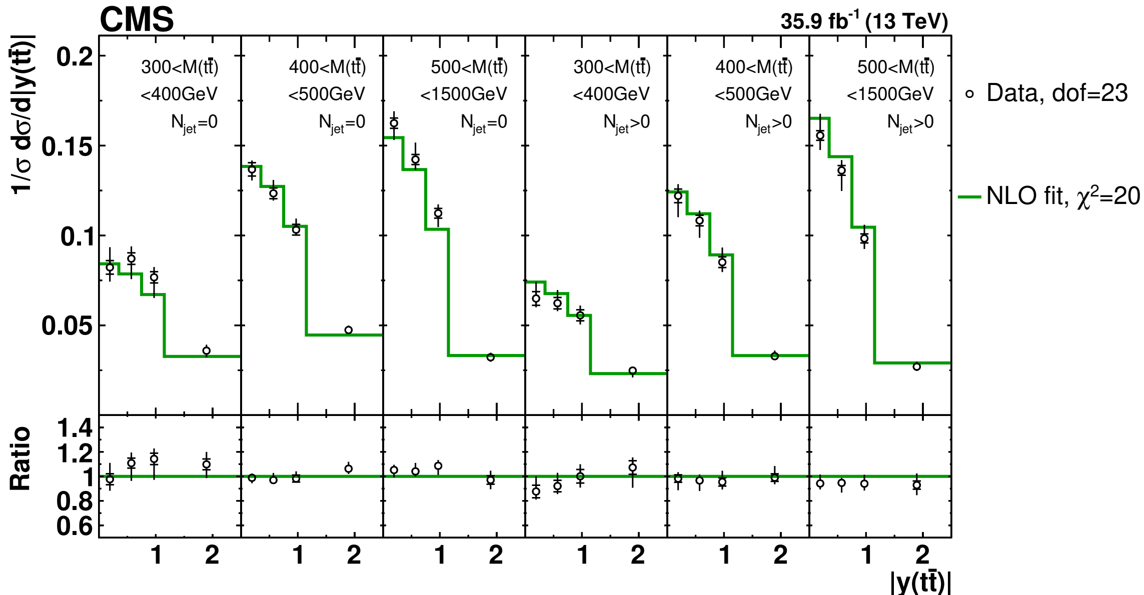

- Measurement of $t\bar{t}$ cross section differential in $M_{t\bar{t}}$, $y_{t\bar{t}}$ and N_{jet} in lepton channel using "loose" kinematic reconstruction.
- NLO QCD analysis using existing PDF sets as well as full PDF fit (using HERA data in addition).
- Data is accurate enough to constrain PDFs, α_S and m_t^{pole} together:

$$\alpha_S(m_Z) = 0.1135 \pm 0.0016(\mathrm{fit})^{+0.0002}_{-0.0004}(\mathrm{model})^{+0.0008}_{-0.0001}(\mathrm{param})^{+0.0011}_{-0.0005}(\mathrm{scale})$$
$$m_t^{pole} = 170.5 \pm 0.7(\mathrm{fit}) \pm 0.1(\mathrm{model})^{+0.0}_{-0.1}(\mathrm{param}) \pm 0.3(\mathrm{scale})\ \mathrm{GeV}$$

CMS, arXiv:1904.05237

Measurement of $\sigma_{t\bar{t}}$ and extraction PDFs+α_S+m_t

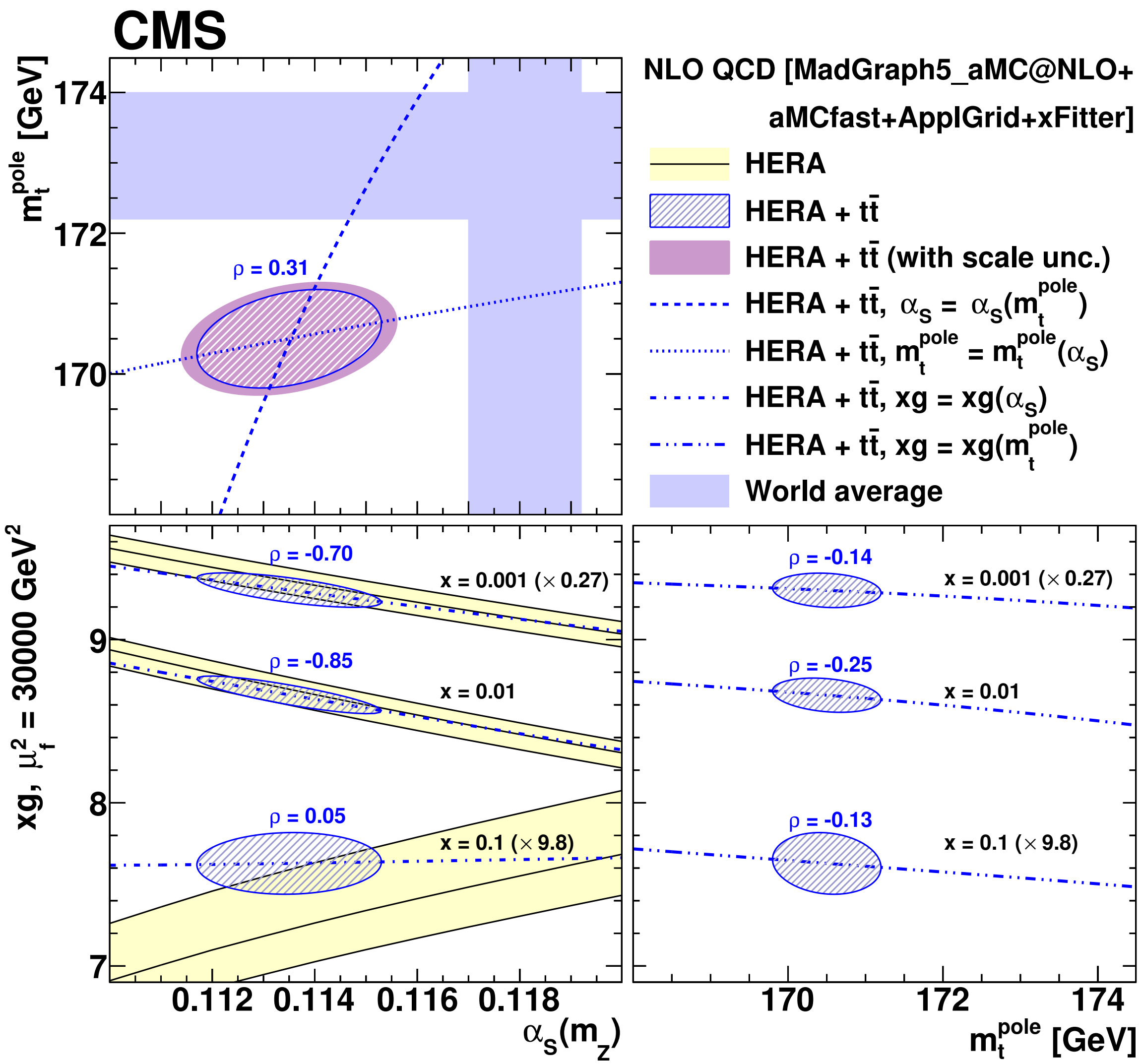

Moderate correlation of the fitted parameters (however remains high for α_S vs gluon at $x = 0.01$).
→ full, consistent NNLO analysis is very interesting.

Combined analysis of jets and $t\bar{t}$

- Combine NLO PDF fit to CMS $t\bar{t}$ and jet data together with HERA. Same 13 TeV data sample, correlations of JES/JER are taken into account

- Good description of the CMS data, with partial χ^2/N_{point} close to unity.

$$\alpha_S(m_Z) = 0.1177 \pm 0.0014(\text{fit}) \pm 0.0022(\text{model and param})$$
$$m_t^{pole} = 170.2 \pm 0.6(\text{fit}) \pm 0.1(\text{model and param})\ \text{GeV}$$

Scale uncertainties are estimated as an envelope of $(\mu_f, \mu_r) = (2, 1/2), (1/2, 2)$ variations and included in model and param uncertainties. Results consistent with the fit to $t\bar{t}$ data only, with reduced uncertainties.

$\rightarrow$ interesting trend that both α_S and m_t tend to be lower in cross secection based extraction vs world average. Full NNLO analysis is required.

Questions for the evening session

- What makes the measurement of the W mass difficult at the LHC? Is it more difficult vs Tevatron?
- Why the measurement of the Z mass is in fact also difficult at the LHC?
- Why data unfolding is required? In which cases it has large/small impact on the result?
- Which processes at the LHC can be used to measure s-quark distribution?
- What is the optimal jet radius for anti-kt jets at the LHC to reduce non-perturbative corrections?
- Why PDF profiling procedure yields in formally correct from the DGLAP point of view PDFs?